Turnpike property in optimal microbial metabolite production

Jean-Baptiste Caillau, Walid Djema, Jean-Luc Gouzé, Sofya Maslovskaya, Jean-Baptiste Pomet

Turnpike property in optimal microbial metabolite production

J.-B. Caillau · W. Djema · J.-L. Gouzé · S. Maslovskaya · J.-B. Pomet

August, 2021

Abstract We consider the problem of maximization of metabolite production in bacterial cells formulated as a dynamical optimal control problem (DOCP). By Pontryagin's maximum principle, optimal solutions are concatenations of singular and bang arcs and exhibit the chattering or *Fuller* phenomenon, which is problematic for applications. To avoid chattering, we introduce a reduced model which is still biologically relevant and retains the important structural features of the original problem. Using a combination of analytical and numerical methods, we show that the singular arc is dominant in the studied DOCPs and exhibits the *turnpike* property. This property is further used in order to design simple and realistic sub-optimal control strategies.

Keywords biological systems · Fuller phenomenon · turnpike property

Mathematics Subject Classification (2000) 49K15 · 92C45

1 Introduction

Microbial species seek to spread as much as possible, according to the availability of nutrients and resources in their surroundings, with the ultimate goal of invading their environment. As a result, when resources are limited, competition sets in between these single-cell organisms which naturally seek to keep themselves alive and develop faster than other competitors. This Darwinian adaptation capacity defines the fitness degree of each microorganism. Such a process can be formulated as a maximization problem of the microbial growth rate in order to outgrow the competitors. The microbial growth is described by ordinary differential equations and the so-called self-replicator model, which is commonly used to study the problems of resources allocation in microorganisms [13, 20, 11], under the assumption that microbial species aim to optimally use their available energy to grow. This results in several applications in biotechnology, where the fitness of bacteria is used to optimize the production of high valuated compounds. Our work fits into this perspective, by developing novel theoretical and synthetic approaches for biotechnological applications. In this specific research area, optimal control theory has greatly contributed to achieving a better understanding of natural biological phenomena, and more importantly, to effectively controlling artificial cultures of microorganisms in biotechnological applications. Theoretical tools such as Pontryagin's Maximum Principle (PMP, [16]) are usually combined with numerical ones like the shooting method or direct optimization approaches [2, 3], in order to provide satisfactory solutions to challenging optimization problems (DOCPs). The difficulty stems mainly from the strong nonlinearities of the models involving biological and chemical constraints. The *turnpike* phenomenon, which states that under some conditions the optimal solution of a given DOCP remains most of the time *'close'* to an optimal steady-state, solution of an associated *static*-OCP

Sofya Maslovskaya, Corresponding author
Department of Mathematics, Paderborn University sofyam@math.uni-paderborn.de

Walid Djema, Jean-Luc Gouzé
Université Côte d'Azur, Inria walid.djema@inria.fr, jean-luc.gouze@inria.fr

Jean-Baptiste Caillau
Université Côte d'Azur, CNRS, Inria, LJAD jean-baptiste.caillau@univ-cotedazur.fr

Jean-Baptiste Pomet
Université Côte d'Azur, Inria, CNRS, LJAD jean-baptiste.pomet@inria.fr,

(see, *e.g.*, [18]), is expected to provide new insights into the DOCP itself. In particular, the *static* solution is easier to determine and also to implement in practice. The concept of turnpike has been recently revisited in the literature and is gaining major attention within the area of optimal control [18,19,9] due to its various applications and validity for different classes of problems. In particular, these phenomena have been reported notably in DOCP dealing with the growth of microorganisms in biotechnological systems [23,7,10]. Among various approaches that describe the turnpike behaviour of the optimal solutions, one can cite measure type estimates as in [10] (*measure turnpike*) and exponential estimate as in [18] (*exponential turnpike*). In our case, we show that the *exponential turnpike* property hold and use it to devise sub-optimal control strategies.

The contributions of the paper go in several directions. First we show that the local exponential turnpike property holds on singular arcs. In contrast to known results on exponential turnpike in [18], we deal with singular trajectories.Using Pontryagin Maximum Principle and hyperbolic properties of the Hamiltonian system verified by extremals, we prove the turnpike property in the same manner as in [18,7]. Note that this result is in line with [7] where the turnpike property is shown for singular trajectories, but different since in our case the singular trajectories are of order two which strongly influences the extremal structure. Singular arcs play a major role in the solutions of the considered DOCP as was discussed in [21] and as can be seen on Fig. 5. Turnpike properties of singular arcs together with the stability of the static control allows us to construct a sub-optimal control strategy by replacing the complicated singular control by a very simple constant control equal to the static control. The contribution of the paper is related to the Fuller phenomenon. It is well known (see, *e.g.*, [24]) that the connection between bang arcs and singular arcs of intrinsic order two can only be achieved through chattering, that is by an infinite number of switchings between bang arcs over a finite time interval. This is problematic for applications and requires some approximation process, see for instance [6]. To tackle this issue we reduce the problem to a simpler one which is biologically relevant and preserves most of the system structure while having the advantage of reducing the order of the single arcs by one. Consequently, the connections between the new optimal control regime no longer requires chattering. Analysis of the reduced problem can be used to derive the turnpike property of the original problem since we also show that the singular flow of the two problems coincide. Thus, we construct a sub-optimal open loop control law that exploits the turnpike property, with the benefits of avoiding chattering of the original solutions.

The paper is organized as follows. In Sect. 2, we introduce the full and reduced models of metabolite production and we state the DOCPs of interest. In Sect. 3, we present some numerical illustrations highlighting the turnpike feature of the optimal solutions. Then, in Sect. 4, we focus on singular flow in the reduced DOCP, and we prove the turnpike property along the singular trajectories. Sect. 5 is devoted to the turnpike property of singular trajectories in the full DOCP. Finally, in Sect. 6, we develop numerical algorithms to solve both problems that are based on singular arcs approximations by constant controls. The numerical results are detailed in Sect. 7.

2 Model of metabolite production

The extended self-replicator model that we consider was proposed by [11], this is a coarse-grained model of resource allocation in bacteria. The cell dynamics comprises the gene expression machinery and the metabolic machinery including production of some metabolite of interest. It also includes an external control which determines the proportion of resources allocated between the gene expression and the metabolic machinery. The key elements in the reactions of the considered model are external substrate S, precursor metabolites P, gene expression machinery R, metabolic machinery M, metabolite of interest X, volume $\mathcal{V} = \beta(M+R)$, where β represents the inverse of the cytoplasmic density. For the sake of simplicity, quantities of the system are expressed as concentrations, *i.e.*, $p = \frac{P}{\mathcal{V}}$, $r = \frac{R}{\mathcal{V}}$, $m = \frac{M}{\mathcal{V}}$, $s = \frac{S}{\mathcal{V}_{ext}}$, $x = \frac{X}{\mathcal{V}}$, where p, r and m are intracellular concentrations of precursor metabolites, ribosomes and metabolic enzymes respectively, s is the extracellular concentration of substrate with respect to a constant external volume $\mathcal{V}_{ext}$. The dynamics of m can be expressed in terms of r and therefore is excluded from the analysis.

2.1 The full model

The general form of the model can be found in [11,23]. Following the modeling steps in [23,11], the synthesis rates in the dynamics are further taken as Michaelis-Menten kinetics. This leads to different models depending on environmental conditions. In our case we restrict our attention to the constant environmental conditions, when s is constant. We are led to the following control system with $u \in [0,1]$ the control function representing the

proportion of resources allocated to gene expression (r), while $1-u$ is allocated to metabolism (m) which is excluded from the system,

$$\begin{cases} \dot{p} = E_M(1-r) - k_1 \frac{p(1-r)}{K_1+p} - (p+1)\frac{pr}{K+p}, \\ \dot{r} = (u-r)\frac{pr}{K+p}, \\ \dot{x} = k_1 \frac{p(1-r)}{K_1+p} - \frac{pr}{K+p}x, \\ \dot{\mathcal{V}} = \frac{pr}{K+p}\mathcal{V}, \end{cases} \tag{1}$$

with constant parameters E_M, K, K_1, k_1 and $p, r, x, \mathcal{V}$ satisfying, $0 < p,\ 0 < x,\ 0 < \mathcal{V},\ 0 \leq r \leq 1$. Control u is assumed to be a measurable function $u : [0, T] \to [0, 1]$. We denote by $\mathcal{U}$ the set of such control functions and call $\mathcal{U}$ the set of admissible controls. Thus, we are interested in maximization of the total quantity of the metabolite of interest X produced during time T using the resource allocation u. For this, we introduce the cost function, $J_X(u) = X(T) - X_0$, with $X_0 = X(0)$ given. Using the dynamics of $x, \mathcal{V}$ in (1), the cost can be expressed in variables (p, r, x) as follows,

$$J_X = \int_0^T \frac{k_1}{x(t)} \frac{p(t)(1-r(t))}{K_1 + p(t)} \mathrm{d}t, \tag{2}$$

where $(p(t), r(t), x(t))$ satisfy (1) for any $t \in [0, T]$. Notice that the dynamics of (p, r, x) do not depend on $\mathcal{V}$. We are led to the following optimal control problem. Find a control $u(\cdot) \in \mathcal{U}$ which maximizes $J_X(u)$ for given T and (p, r, x) satisfying,

$$\begin{cases} \dot{p} = E_M(1-r) - k_1 \frac{p(1-r)}{K_1+p} - (p+1)\frac{pr}{K+p}, \\ \dot{r} = (u-r)\frac{pr}{K+p}, \\ \dot{x} = k_1 \frac{p(1-r)}{K_1+p} - \frac{pr}{K+p}x, \end{cases} \tag{3}$$

with given initial point (p_0, r_0, x_0) and free final point at final-time T.
The existence of an optimal solution has already been shown in [23]. The preliminary analysis in [23], [21] showed that the singular arcs are of order two which implies (cf. [24]) that any connection between bang arcs and singular arc is realized by chattering, that is, infinite number of switchings between bang arcs during a finite-time interval. The chattering phenomenon in optimal solution is problematic for application because it can not be directly implemented. To tackle this issue we propose to consider a reduced control system for which most of the structural properties still holds but the chattering phenomenon does not appear in optimal solutions. Notice first that in the model defined by (3) and (2), the control u only appears in the dynamics of r and at the equilibrium of r we have moreover $u = r$. In addition, r appears linearly in the dynamics of p and x and also in the cost (2).

2.2 **The reduced model**

Since r is the only variable whose time-derivative depends on the control, it is rather natural to consider the reduced system where r is no longer a state variable but a *"cheap"* control. This idea, similar to taking velocities as controls instead of forces for a mechanical systems, is standard [12] and also related to the Goh transformation [1]; some authors call *backstepping* the process of deducing a feedback control for the full system from a feedback control for the the reduced system [8]). The new state variables are (p, x) and the reduced system reads,

$$\begin{cases} \dot{p} = E_M(1-r) - k_1 \frac{p(1-r)}{K_1+p} - (p+1)\frac{pr}{K+p}, \\ \dot{x} = k_1 \frac{p(1-r)}{K_1+p} - x\frac{pr}{K+p}. \end{cases} \tag{4}$$

As before, state (p, x) satisfy $0 < p,\ 0 < x$ and control r satisfies $0 \leq r \leq 1$. The new DOCP (5) aims then to find the control r maximizing the cost (2) under the dynamical constraint (4), the state constraint $0 < p,\ 0 < x$ and control constraint $0 \leq r \leq 1$. The initial position $(p(0), x(0))$ is fixed, while $(p(T), x(T))$ is free, *i.e.*,

$$\max_{r \in \mathcal{U}_r} \int_0^T \frac{k_1}{x(t)} \frac{p(t)(1-r(t))}{K_1 + p(t)} \mathrm{d}t \quad \begin{cases} \text{under the constraint of (4)} \\ p(0) = p_0,\ x(0) = x_0,\ 0 < p,\ 0 < x, \end{cases} \tag{5}$$

where $\mathcal{U}_r$ is the set of admissible controls, that is $\mathcal{U}_r = \{r(\cdot) \text{ measurable } :\ 0 \leq r(t) \leq 1,\ t \in [0, T]\}$. We will call this optimal control problem the reduced problem.

3 Numerical examples highlighting the turnpike features

In this section we provide numerical solutions obtained for both full and reduced models with specified parameters. These solutions serve as illustration for the following sections and show what turnpike property of a trajectory may look like. We anticipate on the next sections in two following ways.
- We say that an optimal solution is made of *bang arcs*, when the control is equal to either 1 or 0 (in both the reduced and full problems, the control takes values in $[0, 1]$, where 0 and 1 are the boundary points), and *singular arcs*, when the control takes values in the interior of $[0, 1]$. In the obtained numerical solutions, we distinguish singular or bang arcs by inspection.
- We use the notion of static optimal control problem which is defined in sections 4.2 and 5.
All the numerical solutions are obtained using *direct* numerical methods, which consist in solving a finite-dimensional optimization problem obtained by discretizing the optimal control problem with respect to both time and space; we use the `bocop` [17] software, that efficiently automatizes this procedure.

In this illustrative section, the parameters present in (2), (3), (4), (5) are fixed to:

$$E_M = k_1 = K_1 = K = 1\,.$$

3.1 Turnpike features in the reduced problem of metabolite production

In the reduced optimal control problem (5), we fix the initial condition to $x(0) = p(0) = 1$. Optimal solutions have been computed[1] for various values of T, results are discussed in Fig. 1-2. See conclusions at the end of Sect. 3.2.

T	10	15	18	20	24	26	28	–
t_1	2.47	2.50	2.60	2.62	2.64	2.64	2.65	–
t_2	62.01	6.67	11.67	14.69	16.72	20.73	22.77	–
T	30	35	40	45	50	55	60	65
t_1	2.63	2.64	2.59	2.56	2.52	2.50	2.53	2.52
t_2	26.82	31.85	36.88	41.94	47.00	52.03	57.00	
T	70	80	90	100	120	125	135	150
t_1	2.52	2.40	2.34	2.40	2.40	2.25	2.16	2.10
t_2	67.06	77.12	87.12	97.20	117.36	122.25	132.30	147.60
T	200	230	250	280	300	310	320	–
t_1	2.00	1.84	2.00	1.68	1.80	1.86	1.90	–
t_2	197.60	227.70	248.00	277.76	298.20	308.14	318.08	–

Table 1: Values of the switching-instants t_1, t_2 for different time horizons $[0, T]$, where T ranges from 10 to 320.

3.2 Turnpike features in the full problem of metabolite production

Let us now consider the initial DOCP (3)-(2). We define the associate *static* optimization problem.

$$\begin{cases} E_M(1-r) - k_1\frac{p(1-r)}{K_1+p} - (p+1)\frac{pr}{K+p} = 0, \\ (u-r)\frac{pr}{K+p} = 0, \\ k_1\frac{p(1-r)}{K_1+p} - \frac{pr}{K+p}x = 0, \\ 0 \le \overline{p},\ 0 < \overline{x},\ 0 \le \overline{r} \le 1,\ 0 \le \overline{u} \le 1\} \end{cases} \qquad \max_{(p,r,x,u)} \ \frac{k_1}{x}\frac{p(1-r)}{K_1+p} \qquad (\mathbf{OCP}_{static})$$

Proposition 3.1 *Problem* $\mathbf{OCP}_{static}$ *with parameters* $E_M = k_1 = K_1 = K = 1$*, admits the unique solution. This solution satisfies* $\overline{u} = \overline{r}$*,* $\overline{x} = \frac{\overline{p}(1-\overline{r})}{\overline{pr}}$*,* $\overline{r} = \frac{1}{\overline{p}^2+\overline{p}+1}$*, where* $\overline{p}$ *is the unique* $p > 0$ *maximizing* $\frac{p}{(p+1)(p^2+p+1)}$*.*

[1] Numerical experiments were run on `bocop`, with the following settings: discretization: Euler (implicit, 1-stage, order 1), time steps: 500, Maximum number of iterations: 2000, NLP solver tolerance: 10^{-20}. The values of t_1 and t_2 for each value of T used in Fig. 2 are given in Tab. 1 for completeness.

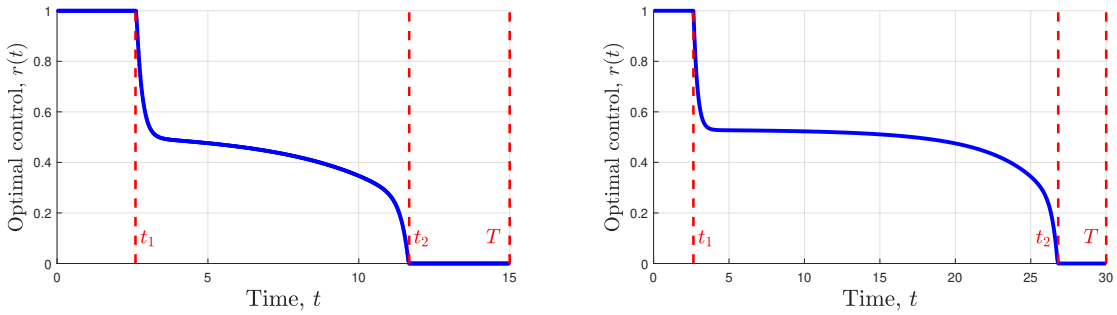

Fig. 1: On the left: the optimal control $r(t)$, $t \in [0, T]$ with $T = 15$. On the right: the optimal control $r(t)$, $t \in [0, T]$ with $T = 30$. The observed optimal control structure is of type ***bang(1)-singular-bang(0)***; we call t_1 the time at the end of the first bang arc and t_2 the time at the end of the second and last one, they are marked on the graphics. One observes that increasing the total duration T seems to increase the duration $t_2 - t_1$ of the singular arc without notably changing the durations t_1 and $T - t_2$ of the bang arcs. This tendency is confirmed in Fig. 2.

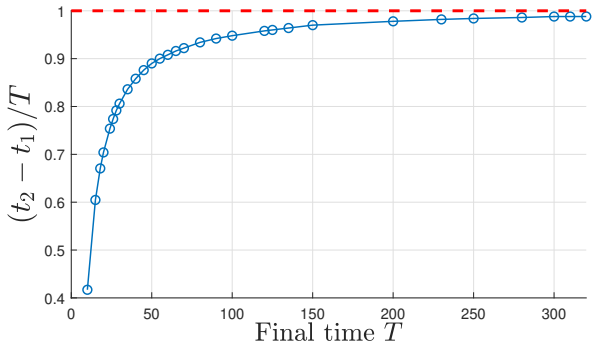

Fig. 2: The same computation as in Fig. 1 has been repeated for various values of T between 10 and 320, t_1 and t_2 have been obtained for each of these values of T (see the table in Footnote 1) and we have plotted the values of $(t_2 - t_1)/T$ against T. This confirms that the time spent on a singular arc becomes drastically preponderant as T becomes large.

Calculating the minimizing $\overline{p} = 0.5652$ from Proposition 3.1, we deduce $\overline{r} = 0.5306$, $\overline{x} = 0.8846$, and $\overline{u} = \overline{r}$. Let us fix the initial conditions to $p(0) = x(0) = 1$ and $r(0) = 1/2$. The optimal trajectories $(p(t), r(t), x(t))$, obtained using the `Bocop` settings[2], are illustrated in Fig. 3 and the optimal control $u(t)$ given in Fig. 4. In Fig. 3, we observe, similarly to the control, that the optimal trajectories evolve around the static point over the time window where the control u is singular (Fig. 4).

The numerical results suggest the following properties:

- the duration of the singular phase increases when we increase the final time T (Fig. 2 and 5),
- the duration of the singular phase increases much faster than the duration of the phase characterized by bang arcs when the time window $[0, T]$ is large,
- for sufficiently large T, the optimal trajectories (Fig. 3) and the optimal control (Fig. 4 and 1) , solutions of the reduced and the full DOCPs, stay most of the time *'close'* to the *static* steady-state solution of the associated *static*-OCPs.

The property of optimal trajectories to stay the most of the time near a steady state when the final time is large enough is well known in control theory and it refers to the *turnpike* phenomenon. Mathematically, *turnpike* can be described in different terms, the most convenient in our case is the approach of [18] where it is characterized via the following estimate at each time $t \in [0, T]$ for $z = (p, r, x)$,

[2] Final time $T = 40$ (time unit), discretization: Midpoint (implicit, 1-stage, order 1), time steps: 7000, Maximum number of iterations: 2000, NLP solver tolerance: 10^{-14}.

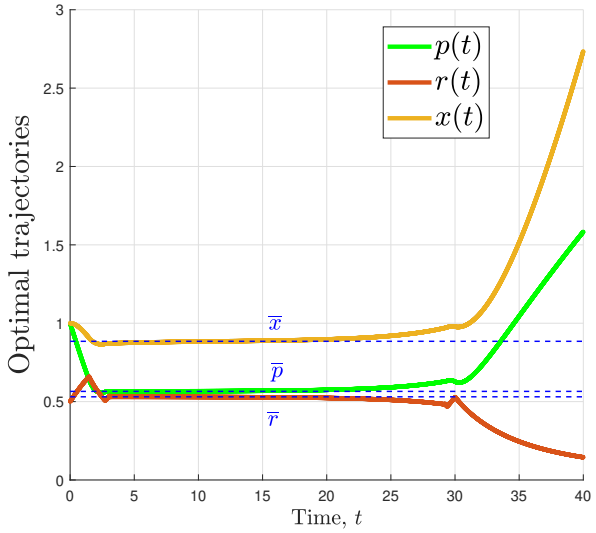

Fig. 3: The optimal trajectories for $t \in [0, 40]$ in the numerical example of Sect. 3.2.

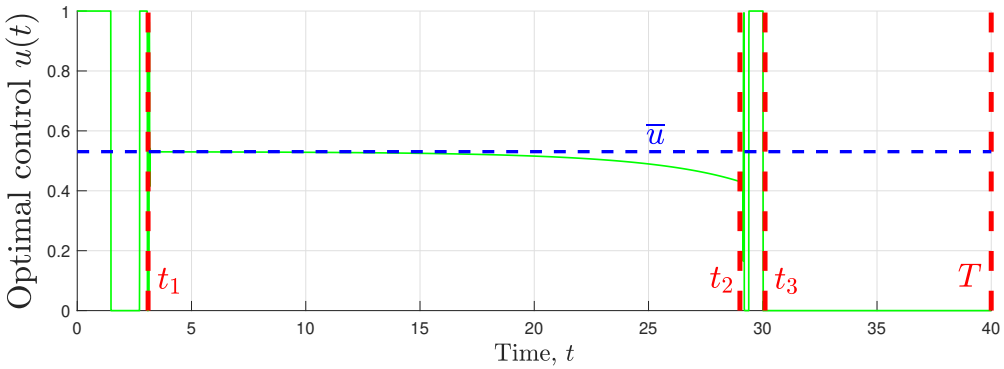

Fig. 4: The optimal control $u(t)$ for $t \in [0, 40]$ in the example of Sect. 3.2.

$$\|u(t) - \bar{u}\| + \|z(t) - \bar{z}\| \leq C \left(e^{-\mu t} + e^{-\mu(T-t)} \right),$$

for some positive parameters μ, C independent from T and for time T large enough. In the following sections we will concentrate on proving the local turnpike property of singular arcs in both reduced and full cases.

4 Turnpike property of the singular flow of the reduced problem

4.1 Reduced problem

Let us start the analysis of the reduced problem defined by (4), (2) by considering the question of existence of optimal solutions. First, for any fixed admissible control function $r(\cdot)$, solution of (4) exists and is well-defined for any $T \in \mathbb{R}^+$ and the set $\{(p, x) \ : \ 0 < p, \ 0 < x\}$ is positively invariant for the system (4), that is, for any initial solution (p_0, x_0) satisfying $0 < p_0, \ 0 < x_0$, the corresponding solution (p, x) of (4) satisfy $0 < p, \ 0 < x$. This can be shown by the same arguments as in [23,22]. The optimal control problem is stated for controls taking values in compact $[0, 1]$ and both integrand of the cost and the dynamics are affine in control. Thus, existence of the optimal solutions is insured by standard Filippov's theorem [1].

To analyse solutions of the reduced problem we apply the PMP [16]. It gives the first order optimality condition and describes the trajectories which are candidates to be optimal solutions. Let us denote by $z^r = (p, x)$ the state,

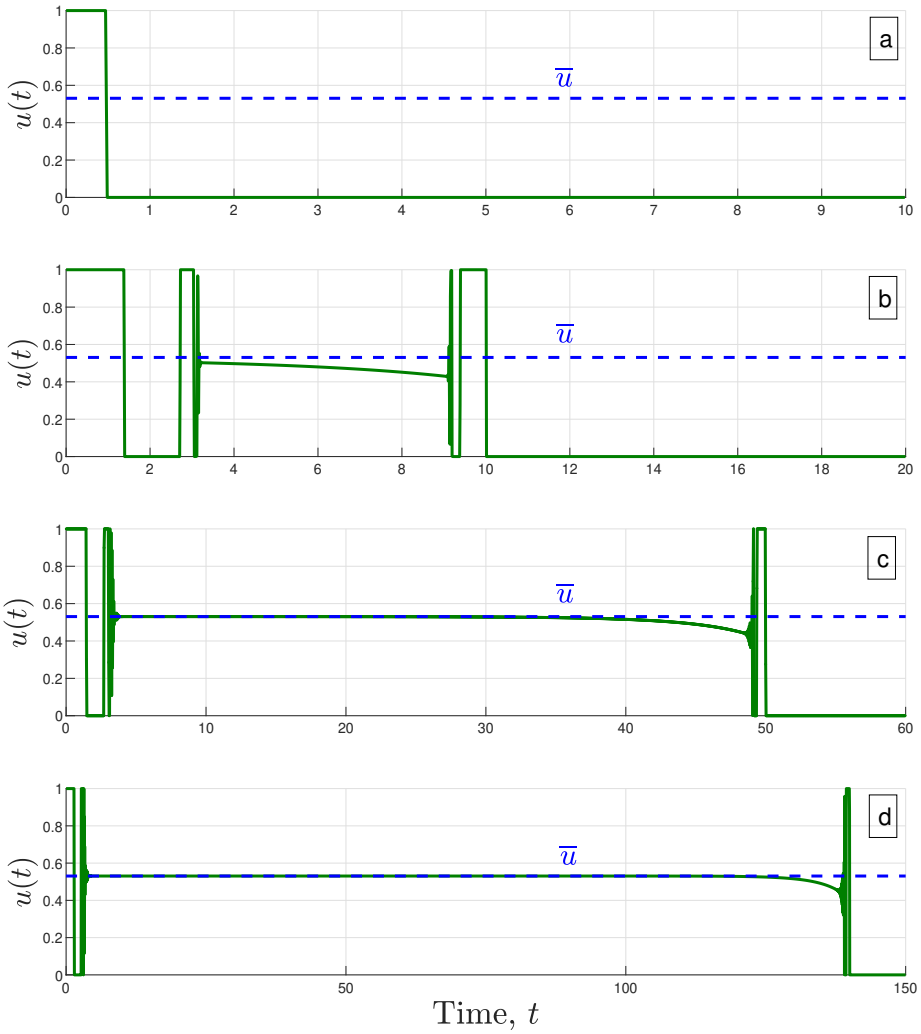

Fig. 5: The singular arc becomes preponderant when T increases.

by $\lambda^r = (\lambda_p, \lambda_x) \in \mathbb{R}^2$ the adjoint state and let $\lambda_0 \leq 0$. We write the cost (2) compactly $J_X = \int_0^T f^0(z, r)$ and denote by $\mathcal{H}^r$ the following function called pseudo-Hamiltonian,

$$\mathcal{H}^r(z, \lambda, \lambda_0, r) = -\lambda_0 \, f_0 + \lambda_p \, \dot{p} + \lambda_x \, \dot{x}.$$

Theorem 4.1 (Pontryagin Maximum Principle) *If $z^r(\cdot)$ is a trajectory of* (4) *which maximizes the cost* (2) *then it is a projection of $(z^r(\cdot), \lambda^r(\cdot), \lambda_0)$ satisfying on $[0, T]$ the following equations,*

$$\begin{cases} \dot{z}^r = \frac{\partial}{\partial \lambda^r} \mathcal{H}^r(z^r, \lambda^r, \lambda_0, \tilde{r}), \\ \dot{\lambda}^r = -\frac{\partial}{\partial z^r} \mathcal{H}^r(z^r, \lambda^r, \lambda_0, \tilde{r}), \\ \mathcal{H}^r(z^r, \lambda^r, \lambda_0, r) = \max_{r \in [0,1]} \mathcal{H}^r(z^r, \lambda^r, \lambda_0, r), \end{cases} \tag{6}$$

and the transversality condition associated with the final condition $(p(T), x(T)) \in \mathbb{R}^n$ (free final condition), $\lambda^r(T) = 0$.

Pair (z^r, λ^r) is called extremal. An extremal is called normal if the associated λ_0 satisfies $\lambda_0 < 0$ and abnormal if $\lambda_0 = 0$. System (6) is invariant under the rescaling of $(\lambda^r(\cdot), \lambda_0)$ by any positive constant and it is standard

to fix $\lambda_0 = -1$ in case of normal extremals. From now on we will write $H^r(z^r, \lambda^r, r)$ for the normal pseudo-Hamiltonian associated with $\lambda_0 = -1$. By the same arguments as in [23] we deduce that the abnormal case $\lambda_0 = 0$ is not possible. This is a consequence of the following properties of the optimal control problem: the dynamics of the adjoint variable $\dot{\lambda}$ is linear in λ and the transversality condition implies $\lambda(T) = 0$.
The reduced control system (4) and $f^0(z, u)$ are affine in control r. Thus, by applying the PMP the corresponding pseudo-Hamiltonian can be written in the following form,

$$H^r(z^r, \lambda^r, r) = H_0^r(z^r, \lambda^r) + r\, H_1^r(z^r, \lambda^r),$$

where the switching function H_1^r is defined as follows,

$$H_1^r = \left(\frac{k_1 p}{p + K_1} - \frac{(p+1)p}{K+p} - E_M\right)\lambda_p - \left(\frac{k_1 p}{p + K_1} + \frac{px}{K+p}\right)\lambda_x - \frac{k_1 p}{x(p + K1)}. \tag{7}$$

From maximization condition in PMP, it follows that the value of the optimal control depends on the values of the switching function H_1^r. The dependence is as follows. If $H_1^r(z^r(t), \lambda^r(t)) > 0$ on some time interval $[a_1, b_1]$ then $r(t) = 1$ on $[a_1, b_1]$; if $H_1^r(z^r(t), \lambda^r(t)) < 0$ on some time interval $[a_2, b_2]$ then $r(t) = 0$ on $[a_2, b_2]$. Finally, if $H_1^r(z^r(t), \lambda^r(t)) = 0$ on some time interval $[a_3, b_3]$ then the corresponding control r is singular on $[a_3, b_3]$. The optimal control is then a concatenation of bang controls $u \equiv 1$, bang controls $u \equiv 0$ and singular controls.

From the transversality condition $\lambda^r(T) = 0$, it follows that $\lambda_p(T) = \lambda_x(T) = 0$. Substituting $\lambda_p(T) = \lambda_x(T) = 0$ in (7) and taking into account $p, x > 0$, we deduce $H_1^r(z(T), \lambda(T)) \neq 0$. By continuity of $H_1^r(t)$, there exists $\epsilon > 0$ such that $H_1^r(t) \neq 0$ for $t \in [T - \epsilon, T]$. This implies that r is not singular on $[T - \epsilon, T]$ which means that any extremal ends with a bang arc. Moreover, from $H_1^r(T) = -\frac{k_1 p}{x(p+K1)} < 0$, we deduce that the final bang control is $r \equiv 0$.

4.2 **Static problem.**

Now let us define the static problem corresponding to (5). In the static problem we are looking for the steady state of the dynamics (4) at which the cost (2) reaches its maximum. Let us denote the dynamics (4) of z^r by $(\dot{z^r}) = f_r(z^r, r)$. The static problem is defined as follows.

$$\max f^0(z^r, r), \quad s.t. \quad \begin{cases} f_r(z^r, r) = 0, \\ 0 < p, x, \quad 0 \leq r \leq 1 \end{cases} \tag{8}$$

Let us define in the same way the static problem corresponding to the original problem defined by (1), (2).

$$\max f^0(z^r, r), \quad s.t. \qquad \begin{cases} f_r(z^r, r) = 0, \;\; (u - r)\frac{pr}{K+p} = 0, \\ 0 < p, x, \quad 0 \leq r, u \leq 1 \end{cases} \tag{9}$$

As $\frac{pr}{K+p}$ is non-negative, the solution of (9) satisfies either $r = 0$ or $u = r$. Both cost and equations in (9) do not depend on u, therefore, in both cases, the optimal value of r coincides with the value optimal for (8). Hence, we proved the following result.

Proposition 4.1 *Solution* (p, x, r) *of the static problem* (9) *coincides with the solution of the static problem* (8).

From the form of $f_r(z^r, r)$ given by (4), r and x can be expressed as rational functions of p and the problem of maximization of $f^0(z^r, r)$ can be reformulated as a problem of maximization of a rational function $f^0(z^r(p), r(p))$ on $p > 0$. It was shown in [23], that the value of p maximising f^0 is unique in the domain $p > 0$ for (9). As a consequence of Proposition 4.1, the same holds for the reduced problem, i.e. for (8). We will call *static point* the solution of the *static*-OCP.

4.3 **Singular flow**

Let us now consider in more details the singular control. First we denote $H_{01}^r = \{H_0^r, H_1^r\}$ and by induction $H_{0i}^r = \{H_0^r, H_i^r\}$ and $H_{1i}^r = \{H_1^r, H_i^r\}$, where i is any sequence of 0s and 1s and $\{\cdot, \cdot\}$ is the Poisson bracket. The singular control is the control corresponding to the case $H_1^r(t) \equiv 0$ on some time interval. The value of singular control can be obtained by differentiating $H_1^r(t) = 0$, see [1,4] for more details. The order of the control

is the smallest number d such that the control u can be expressed from, $\frac{d^{2d}}{dt^{2d}} H_1^r(t) = 0$. In the case of reduced problem, the control can be obtained from, $\frac{d^2}{dt^2} H_1^r(z^r, \lambda^r) = H_{001}^r(z^r, \lambda^r) + r H_{101}^r(z^r, \lambda^r)$. Thus, the singular control is of order 1 and is defined by: $r_s = -\frac{H_{001}^r(z^r,\lambda^r)}{H_{101}^r(z^r,\lambda^r)}$. By [24], if the singular control is of order 1, then the connection between bang control and singular control is a simple connection, that is, not by chattering. Thus, chattering phenomenon does not occur in solutions to reduced problem. The extermal associated with the singular control is called singular and belongs to the singular surface: $\Sigma_r = \left\{(z^r, \lambda^r) \in \mathbb{R}^4 \,|\, H_1^r = 0,\ H_{01}^r = 0\right\}$.

Proposition 4.2 *There exists a neighborhood of $(\bar{p}, \bar{x})$ solution of the static-OCP* (8) *where the singular surface is defined by $(\lambda_p, \lambda_x) = (\lambda_p(p,x), \lambda_x(p,x))$ solution of,*

$$\begin{array}{l} a_1(p,x)\lambda_p + b_1(p,x)\lambda_x = c_1(p,x), \\ a_2(p,x)\lambda_p + b_2(p,x)\lambda_x = c_2(p,x), \end{array} \tag{10}$$

with coefficients $a_1, a_2, b_1, b_2, c_1, c_2$ defined by,

$$\begin{array}{l} H_1(p,x,\lambda_p,\lambda_x) = a_1(p,x)\lambda_p + b_1(p,x)\lambda_x - c_1(p,x), \\ H_{01}(p,x,\lambda_p,\lambda_x) = a_2(p,x)\lambda_p + b_2(p,x)\lambda_x - c_2(p,x). \end{array}$$

Proof. By definition of the singular surface, (λ_p, λ_x) satisfy (10), which admits a unique solution if and only if the matrix $\Delta = \begin{pmatrix} a_1 & b_1 \\ a_2 & b_2 \end{pmatrix}$ is invertible. Let $D = D(p,x)$ be the determinant of Δ. At an equilibrium of (4) we have,

$$x = \frac{(p+1)\mu_1}{E_M - \mu_1}, \quad \text{and} \quad r = \frac{E_M - \mu_1}{E_M - \mu_1 + (p+1)\mu_2}, \tag{11}$$

with $\mu_1 = \frac{k_1 p}{K_1 + p}, \mu_2 = \frac{p}{K+p}$. Let us substitute $x = x(p), r = r(p)$ from (11) in $\Delta(p,x)$ and $f^0(p,r,x)$. Then the following identity obtained using Maple holds,

$$D(p, x(p))\, f^0(p, r(p), x(p)) = \frac{p^2(p+1)E_M k_1 K_1}{(p+K)^2(p+K_1)^2} \neq 0.$$

We conclude that $D(\bar{p}, \bar{x}) \neq 0$. Function $D(p,x)$ is continuous and thus it is different from zero in some neighborhood of $(\bar{p}, \bar{x})$ which implies existence of a unique solution of system (10).

□

Substitution of the singular control r_s in (6) gives

$$\begin{cases} \dot{z^r} = \frac{\partial H}{\partial \lambda^r}(z^r, \lambda^r, r_s(z^r, \lambda^r)), \\ \dot{\lambda^r} = -\frac{\partial H}{\partial z^r}(z^r, \lambda, r_s(z^r, \lambda^r)). \end{cases} \tag{12}$$

For any $(z^r, \lambda^r) \in \Sigma_r$, singular Hamiltonian is defined by,

$$H_s(z^r, \lambda^r) = H(z^r, \lambda^r, r_s(z^r, \lambda^r)).$$

Thus, we can rewrite (12) on Σ_r as follows.

$$\begin{cases} \dot{z}^r = \frac{\partial H_s}{\partial \lambda^r}(z^r, \lambda^r), \\ \dot{\lambda}^r = -\frac{\partial H_s}{\partial z^r}(z^r, \lambda^r). \end{cases} \tag{13}$$

Proposition 4.3 *Singular system* (13) *is Hamiltonian on Σ_r.*

Proof. Let w be the symplectic form defined by the reduced problem (4), (2). In coordinates (z^r, λ^r) we have $w = dz_i^r \wedge d\lambda_i^r$. To be symplectic, $w|_{\Sigma_r}$ should be non-degenerate and closed, i.e. $dw|_{\Sigma_r} = 0$. It is closed by definition of the exterior derivative, so we are left to show that it is non-degenerate. By definition, $w|_{\Sigma_r}$ is non-degenerate if for any $q \in \Sigma_r$ and any $X \in T_q\Sigma_r$ we have $(w(X,Y) = 0 \text{ for all } Y \in T_qM) \Rightarrow (X = 0)$. The tangent bundle $T\Sigma_r$ is defined by,

$$T\Sigma_r = (\operatorname{Ker} dH_1 \cap \operatorname{Ker} dH_{01})|_{\Sigma_r} = (\operatorname{span}\{\mathbf{H}_1, \mathbf{H}_{01}\})^{\perp}\Big|_{\Sigma_r},$$

where $\mathbf{f}$ is defined by $df = w(\mathbf{f}, \cdot)$ for any function $f : \mathbb{R}^4 \to \mathbb{R}$. The symplectic orthogonal $(\mathrm{span}\{\mathbf{H}_1, \mathbf{H}_{01}\})^\perp$ is defined as follows,

$$(\mathrm{span}\{\mathbf{H}_1, \mathbf{H}_{01}\})^\perp = \{X \in \mathbb{R}^4 : w(X, \mathbf{H}_1) = \ w(X, \mathbf{H}_{01}) = 0\}.$$

Symplectic form w is degenerate if and only if $T\Sigma_r \cap T\Sigma_r{}^\perp = 0$, *i.e.*,

$$\mathrm{span}\{\mathbf{H}_1, \mathbf{H}_{01}\} \cap (\mathrm{span}\{\mathbf{H}_1, \mathbf{H}_{01}\})^\perp = 0.$$

We will show that w is non-degenerate by contradiction. Assume there exists a nonzero vector field $X = \alpha\mathbf{H}_1 + \beta\mathbf{H}_{01}$ such that $w(X, \mathbf{H}_1) = 0$ and $w(X, \mathbf{H}_{01}) = 0$. Then $\alpha = 0$ and $\beta = 0$ or $w(\mathbf{H}_1, \mathbf{H}_{01}) = 0$. By definition, $w(\mathbf{H}_1, \mathbf{H}_{01}) = H_{101}$ which is nonzero in our case, so $X = 0$ which contradict our assumption. As a result we showed that $(\Sigma_r, w|_{\Sigma_r})$ is a symplectic manifold. A flow of (13) is Hamiltonian if and only if it preserves $w|_{\Sigma_r}$, see [1]. We have Lie derivative $\mathcal{L}_{\mathbf{H}}\, w|_{\Sigma_r} = i_{\mathbf{H}} \circ dw|_{\Sigma_r} + d \circ i_{\mathbf{H}}\, w|_{\Sigma_r}$ and $i_{\mathbf{H}}\, w|_{\Sigma_r} = i_{\mathbf{H}} w = dH$ as $\mathbf{H}|_{\Sigma_r}$ is a section of $T\Sigma_r$. Therefore, $\mathcal{L}_{\mathbf{H}}\, w|_{\Sigma_r} = 0$ and it completes the proof of the Proposition. □

4.4 **Turnpike theorem.**

The main result of this section is given by Theorem 4.2, in which we show local exponential turnpike property of a singular trajectory, solution of (13). We assume that a solution of (13) is well defined on a time interval $[t_1, t_2]$.

Theorem 4.2 *There exists a positive constant ϵ such that, if $z^r(\cdot)$ is singular and satisfies* (13) *on $[t_1, t_2]$, $\bar{z}_r$ is the solution of static OCP* (8)*, and if*

$$\|z^r(t_1) - \bar{z}_r\| + \|z^r(t_2) - \bar{z}^r\| \leq \epsilon$$

then there exists $C > 0$ such that for any $t \in [t_1, t_2]$ there holds

$$\|z^r(t) - \bar{z}_r\| + |r_s(t) - \bar{r}| \leq C\left(e^{\mu(t_1 - t)} + e^{\mu(t - t_2)}\right) \tag{14}$$

where $\mu = \frac{\bar{p}\bar{r}}{K+\bar{p}}$.

The singular arc belongs to 2-dimensional surface Σ_r and, by Proposition 4.2, can be parameterized by (p, x) near the solution of the static problem $(\bar{p}, \bar{x})$. Notice that the singular control of the reduced problem r_s is a function only of p, and thus, we can rewrite the singular system as follows,

$$\begin{cases} \dot{p} = f_p(p), \\ \dot{x} = f_r(p) - \frac{pr(p)}{K+p}\, x. \end{cases} \tag{15}$$

Let us introduce perturbations of the singular arc on Σ_r near $(\bar{p}, \bar{x})$,

$$\delta p = p(t) - \bar{p} \quad \delta x = x(t) - \bar{x}, \quad \delta r = r(t) - \bar{r}. \tag{16}$$

Be definition, $(\delta p, \delta x)$ satisfy,

$$\frac{d}{dt}\begin{pmatrix} \delta p \\ \delta x \end{pmatrix} = \mathcal{H}\begin{pmatrix} \delta p \\ \delta x \end{pmatrix} + \begin{pmatrix} o_1(\delta p, \delta x) \\ o_2(\delta p, \delta x) \end{pmatrix} \quad \text{with} \quad \mathcal{H} = \begin{pmatrix} * & 0 \\ * & -\frac{\bar{p}\bar{r}}{K+\bar{p}} \end{pmatrix} \tag{17}$$

and o_1, o_2 are C^1 functions on some neighborhood of $(0, 0) \in \mathbb{R}^{2n}$ which have a little-o behavior, in our framework we will use the following definition of little-o functions:

$$\frac{\|o(x, y)\|}{\|(x, y)\|} \xrightarrow[(x,y)\,\to\,0]{} 0 \qquad (x, y) \in \mathbb{R}^{2n}. \tag{18}$$

The linear part of (17) defines the linearized system,

$$\frac{d}{dt}\begin{pmatrix} \delta p \\ \delta x \end{pmatrix} = \mathcal{H}\begin{pmatrix} \delta p \\ \delta x \end{pmatrix}. \tag{19}$$

Lemma 4.1 *Matrix $\mathcal{H}$ is hyperbolic with opposite eigenvalues.*

Proof. Consider the linearized system (19) in canonical coordinates,

$$\frac{d}{dt}\begin{pmatrix}\delta z_s\\ \delta\lambda_s\end{pmatrix} = \mathcal{H}_s\begin{pmatrix}\delta z_s\\ \delta\lambda_s\end{pmatrix}, \tag{20}$$

where $\mathcal{H}_s$ is (2×2) matrix of the form,

$$\mathcal{H}_s = \begin{pmatrix} \frac{\partial^2 h_s}{\partial\lambda_s\partial z_s}(\bar z_s,\bar\lambda_s) & \frac{\partial^2 h_s}{\partial\lambda_s^2}(\bar z_s,\bar\lambda_s)\\ \frac{\partial^2 h_s}{\partial z_s^2}(\bar z_s,\bar\lambda_s) & -\frac{\partial^2 h_s}{\partial\lambda_s\partial z_s}(\bar z_s,\bar\lambda_s)\end{pmatrix}.$$

The matrix $\mathcal{H}_s$ is traceless by construction and so is $\mathcal{H}$ as trace is invariant under a change of basis. Therefore, eigenvalues of $\mathcal{H}$ are μ and $-\mu$ with,

$$\mu = \frac{\bar p\bar r}{K+\bar p} > 0.$$

□

As $\mathcal{H}$ is hyperbolic, there exists a change of coordinates,

$$\begin{pmatrix} g\\ h\end{pmatrix} = \begin{pmatrix} a_{1,1}\ a_{1,2}\\ a_{2,1}\ a_{2,2}\end{pmatrix}\begin{pmatrix}\delta p\\ \delta x\end{pmatrix},$$

such that (19) in these coordinates takes the following form,

$$\frac{d}{dt}\begin{pmatrix} g\\ h\end{pmatrix} = \begin{pmatrix} -\mu & 0\\ 0 & \mu\end{pmatrix}\begin{pmatrix} g\\ h\end{pmatrix} + \begin{pmatrix}\tilde o_1(g,h)\\ \tilde o_2(g,h)\end{pmatrix}. \tag{21}$$

Lemma 4.2 *[15] For any $T>0$ there exists $\rho>0$ such that the following two statements hold.*

- *For any $(g_0,h_T)\in B(0,\frac{\rho}{K})$ there exists the unique $(g,h)\in C^1\left([0,T],\mathbb{R}^2\right)$ satisfying* (21) *and,*

$$\begin{cases} g(0)=g_0, \quad h(T)=h_T,\\ |g(t)|+|h(t)|\le\rho, \quad t\in[0,T].\end{cases}$$

- *The map Φ defined by $\Phi(g_0,h_T)=(g(\cdot),h(\cdot))$ is continuous.*

Lemma 4.3 *[15] Let $\mu\in\mathbb{R}_+$ be the positive eigenvalue of $\mathcal{H}$. There exists $r_\mu\in(0,\infty)$ independent of $T\in(0,\infty)$ and functions $\theta_1,\theta_2\in C_0\left([0,\bar r_\mu];\mathbb{R}_+\right)$ satisfying $\theta_i(\beta)\xrightarrow[\beta\to 0+]{}0$ for $i=1,2$, such that if (g,h) satisfies* (21) *and*

$$|g(t)|+|h(t)|\le r_\mu, \qquad t\in[0,T],$$

then for any $t\in[0,T]$ there holds

$$\begin{cases} |g(t)|\le C_\mu\left(|g(0)|\ e^{-\mu t}+e^{-\mu(T-t)}\ |h(T)|\ \theta_1(\|h\|_{c^0})\right),\\ |h(t)|\le C_\mu\left(|h(T)|\ e^{-\mu(T-t)}+e^{-\mu t}\ |g(0)|\ \theta_2(\|g\|_{c^0})\right).\end{cases} \tag{22}$$

Proof of Theorem 4.2. By Proposition 4.2, there exists a neighborhood $V\subset\mathbb{R}^2$ of $\bar z_r$ such that in this neighborhood solutions of (13) can be parameterized by (p,x) and satisfy (15). Let us choose $\tilde\epsilon$ such that z^r satisfying $\|z^r-\bar z_r\|\le\tilde\epsilon$ belong to V. We consider the perturbed system (19). Applying Lemmas 4.2, 4.3 to the diagonalized system (21), we have existence of $r_\mu>0$ such that if

$$\begin{cases} g(0)=a_{1,1}\,p(0)+a_{1,2}\,x(0),\\ h(T)=a_{2,1}\,p(T)+a_{2,2}\,x(T)\end{cases} \tag{23}$$

satisfy $|g(0)|+|h(T)|\le r_\mu$ then $(g(t),h(t))$ satisfy (22) for $t\in[0,T]$ and any final time T. Coming back to the initial coordinates $(\delta p,\delta x)$, if,

$$|p(0)|+|x(0)|+|p(T)|+|x(T)|\le\|A\|\,r_\mu,$$

then,

$$|\delta p(t)| + |\delta x(t)| \leq \|A\|^{-1} \left(|g(t)| + |h(t)|\right),$$

and as (22) applies, there exists a positive constant C such that,

$$|\delta p(t)| + |\delta x(t)| \leq C \left(e^{\mu(t_1 - t)} + e^{\mu(t - t_2)}\right).$$

Note that there exists $R = R(r_\mu)$ *s.t.* $\|\delta p(t)\| + \|\delta x(t)\| \leq R$ for all $t \in [0, T]$. Along the singular arc, r is a continuous function of (p, x), thus we get for δr

$$|\delta r(t)| \leq \sup_{B((\bar{p},\bar{x}),R)} |\nabla_p\, r|\, |\delta p| + \sup_{B((\bar{p},\bar{x}),R)} |\nabla_x\, r|\, |\delta x|.$$

As a conclusion, up to a change of constant C, we obtain (14) which ends the proof. □

The obtained result concerns the singular trajectory, which may be a part of the optimal solution. What about the whole solution? The numerical results obtained in Section 3.1 suggest that when the final time is big enough, any optimal solution contains a singular arc. Moreover, the singular arc constitutes the major part of a solution and this part grows relatively to the other part of trajectory when we increase the final time as was shown in Fig. 1. As a result, numerical examples show that the turnpike occurs not only at the level of the singular arc but for the whole trajectory. These observations lead us to the following conjecture.

Corollary 4.3. *Fix (p_0, x_0) in $(0, +\infty) \times (0, +\infty)$. There exists a constant $T_0 > 0$ such that for any $T > T_0$ and any optimal extremal $t \mapsto (z_r(t), \lambda_r(t))$ for problem* (4)-(5) *with initial condition (p_0, x_0), and with associated control $t \mapsto r(t)$, the following upper-bound holds for any t in $[0, T]$:*

$$\|z_r(t) - \bar{z}\| + |r(t) - \bar{r}| \leq C \left(e^{-\mu t} + e^{\mu(t-T)}\right).$$

5 Turnpike property of the singular flow of the original problem

Let us now come back to the original optimal control problem given by dynamics (3) and cost (2). The first steps in the analysis of this optimal control problem were done in [23]. In particular, they showed the existence of optimal solutions and using `Bocop`, they obtained numerical result showing the turnpike behavior of solutions. We will go further in this section and show analytically that the singular arcs, parts of the extremal associated with the singular control, admit the local turnpike property.

We denote by $z = (p, r, x)$ the state, by $\lambda = (\lambda_p, \lambda_r, \lambda_x) \in \mathbb{R}^3$ the adjoint state. We denote by $\mathcal{H}$ the pseudo-Hamiltonian associated with (3) and cost (2),

$$\mathcal{H}(z, \lambda, u) = f_0 + \lambda_p\, \dot{p} + \lambda_r\, \dot{r} + \lambda_x\, \dot{x}.$$

It can be also written alternatively as an affine function of the control u,

$$\mathcal{H}(z, \lambda, u) = H_0(z, \lambda) + u\, H_1(z, \lambda).$$

From PMP, each optimal z satisfies the generalized Hamiltonian system,

$$\begin{cases} \dot{z} = \frac{\partial}{\partial \lambda} \mathcal{H}(z, \lambda, \tilde{u}), \\ \dot{\lambda} = -\frac{\partial}{\partial z} \mathcal{H}(z, \lambda, \tilde{u}), \\ \mathcal{H}(z, \lambda, \tilde{u}) = \max_{u \in [0,1]} \mathcal{H}(z, \lambda, u). \end{cases} \tag{24}$$

Each solution of (24) is a concatenation of bang and singular arcs, where by arcs we mean the parts of the trajectory, singular arc is associated with singular control on the corresponding time interval, bang arc is associated with the bang control.

5.1 **Singular flow**

Let us focus on the singular arcs. It was shown in [23,21] that the singular controls are of order 2. By [24], the connection between singular control of order 2 and bang control can be achieved only by chattering. The singular control is of order 2, and thus, it can be obtained from $\frac{d^4}{dt^4}H_1(t) = 0$, which leads to,

$$u_s = -\frac{H_{00001}(z,\lambda)}{H_{10001}(z,\lambda)}.$$

The corresponding singular extremals belongs to the singular surface defined by,

$$\Sigma = \left\{(z,\lambda) \in \mathbb{R}^6 \,|\, H_1 = 0,\ H_{01} = 0,\ H_{001} = 0,\ H_{0001} = 0\right\}.$$

As in the reduced problem, we substitute the expression of u_s as a function of (z,λ) in $\mathcal{H}(z,\lambda,u)$ and obtain singular Hamiltonian $H_s(z,\lambda) = \mathcal{H}(z,\lambda,u_s(z,\lambda))$. The system (24) becomes accordingly

$$\begin{cases} \dot{z} = \frac{\partial H_s}{\partial \lambda}(z,\lambda), \\ \dot{\lambda} = -\frac{\partial H_s}{\partial z}(z,\lambda). \end{cases} \tag{25}$$

The flow of this system is the singular flow. Understanding properties of singular flow, we understand the properties of singular arcs, parts of optimal solution.

Proposition 5.1 *Singular system* (25) *is Hamiltonian on* Σ.

Proof. Let us show that w defined by $w = dz_i \wedge d\lambda_i$ restricted to Σ is symplectic. In this case we have,

$$T\Sigma = \left(\mathrm{span}\{\mathbf{H}_1, \mathbf{H}_{01}, \mathbf{H}_{001}, \mathbf{H}_{0001}\}\right)^{\perp}\Big|_{\Sigma}.$$

We use the same kind of arguments as in Proposition 4.3 and assume that there exists nonzero vector field $X = \alpha_1\mathbf{H}_1 + \alpha_2\mathbf{H}_{01} + \alpha_3\mathbf{H}_{001} + \alpha_4\mathbf{H}_{0001}$ such that $w(X,\mathbf{H}_1) = 0,\ w(X,\mathbf{H}_{01}) = 0,\ w(X,\mathbf{H}_{001}) = 0,\ w(X,\mathbf{H}_{0001}) = 0$. In this case it implies the following system of equations

$$\begin{pmatrix} 0 & H_{101} & H_{1001} & H_{10001} \\ -H_{101} & 0 & \{H_{01},H_{001}\} & * \\ -H_{1001} & -\{H_{01},H_{001}\} & 0 & * \\ -H_{10001} & * & * & 0 \end{pmatrix} \begin{pmatrix} \alpha_1 \\ \alpha_2 \\ \alpha_3 \\ \alpha_4 \end{pmatrix} = 0$$

The system above admits a nontrivial solution if and only if the corresponding matrix is non-degenerate. By applying Jacobi identity to H_{1001}, we get $H_{1001} = \{H_0, H_{101}\}$. Taking into account that $H_{101} = \frac{p}{p+K}H_{01}$, we get $H_{1001} = a_1(z)H_{01} + a_2(z)H_{001} = 0$ for some functions a_1, a_2 smooth on the domain of definition. Next, applying the Jacobi identity to $\{H_{01}, H_{001}\}$ we get $\{H_{01}, H_{001}\} = H_{01001} - H_{10001}$. Using the same arguments as before, we get $H_{01001} = b_1(z)H_{01} + b_2(z)H_{001} + b_3(z)H_{001} = 0$. Taking into account all the zero terms, the matrix above can be written in the following triangular form

$$\begin{pmatrix} 0 & 0 & 0 & H_{10001} \\ 0 & 0 & -H_{10001} & * \\ 0 & H_{10001} & 0 & * \\ -H_{10001} & * & * & 0 \end{pmatrix}$$

which is of full rank in case $H_{10001} \neq 0$. This condition holds for singular trajectories of order two, and thus, for all singular trajectories in our case. This proves that $X = 0$ which contradicts the initial assumption and proves that w restricted to Σ is symplectic. This implies that singular flow is Hamiltonian, we refer to Proposition 4.3 for this final step of the proof. □

We will now establish a relation between the singular flow of the original optimal control problem given by dynamics (3) and cost (2) and the singular flow of the reduced problem (5).

Theorem 5.1 *If the singular control u_s satisfies $0 < u_s < 1$, then singular trajectory $(p(\cdot), r(\cdot), x(\cdot))$ of OCP* (1), (2) *coincides with $(\tilde{p}(\cdot), \tilde{r}(\cdot), \tilde{x}(\cdot))$ where $\tilde{r}(\cdot)$ is the singular control and $(\tilde{p}(\cdot), \tilde{x}(\cdot))$ is the singular trajectory of* (5)*. Moreover, the singular surface of OCP* (1)*,* (2) *can be written as follows*

$$\Sigma = \left\{(p, r, x, \lambda_p, \lambda_r, \lambda_x) \in \mathbb{R}^6 \mid (p, x, \lambda_p, \lambda_x) \in \Sigma_r,\ \lambda_r = 0,\ r = r_s\right\}. \tag{26}$$

Proof. A trajectory of (1), (2) is singular if and only if the following equality holds along the trajectory, $H_1 = \frac{\lambda_r p r}{K+p} = 0$. As we are restricted to the domain $0 < p, 0 < r < 1$, the equality holds if and only if $\lambda_r = 0$. Now notice that there holds, $\mathcal{H} = H_0^r + r\, H_1^r + H_1\,(u - r)$, and therefore,

$$\frac{\partial \mathcal{H}}{\partial r} = H_1^r + \lambda_r \frac{p}{K+p}(u - 2r). \tag{27}$$

Let us differentiate $\lambda_r = 0$ along singular solutions of (24). Using (27), we get,

$$\begin{aligned}
\frac{d}{dt}\lambda_r &= -\frac{\partial \mathcal{H}}{\partial r}\bigg|_{\lambda_r = 0} = -H_1^r = 0, \\
\frac{d^2}{dt^2}\lambda_r &= -\frac{d}{dt}\left(\frac{\partial \mathcal{H}}{\partial r}\right)\bigg|_{\lambda_r = 0, \dot{\lambda}_r = 0} = -\frac{d}{dt}\left(H_1^r\right) = 0, \\
\frac{d^3}{dt^3}\lambda_r &= -\frac{d^2}{dt^2}\left(\frac{\partial \mathcal{H}}{\partial r}\right)\bigg|_{\lambda_r = 0, \dot{\lambda}_r = 0, \ddot{\lambda}_r = 0} = -\frac{d^2}{dt^2}\left(H_1^r\right) = 0.
\end{aligned} \tag{28}$$

Now notice that the first two equations from (28) are equivalent to (10), and define the condition $(p, x, \lambda_p, \lambda_x) \in \Sigma_r$. The last equation from (28) can be written as,

$$\frac{d^2}{dt^2}\left(H_1^r\right) = H_{001} + r\, H_{101},$$

thus, r satisfying this equation is exactly the singular control r_s. On the other hand, the left-hand side of (28) together with $\lambda_r = 0$ defines the singular surface of the initial OCP problem and so we get (26). Now it is sufficient to notice that the dynamics of (p, x) in (1) does not depend on u, but depend on r which is given by $r = r_s$. □

Moreover, near the static point, Σ can be expressed in a simple way.

Proposition 5.2 *Near the solution of the static problem* (8) *the singular surface Σ can be parameterized by $z^r = (p, x)$ and the singular extremal is the solution of Hamiltonian system,*

$$\dot{z^r} = f(z^r, r_s(z^r)).$$

Proof. Using Proposition 4.2, we have $\lambda_p = \lambda_p(p, x), \lambda_x = \lambda_x(p, x)$ and moreover we have $r = r_s(p, x)$, thus Σ is parameterized by (p, x). □

Remark 5.1 Symbolic calculations using Maple show that the singular control $r = r_s(p, x)$ is independent of x, that is $r_s = r_s(p)$.

5.2 **Turnpike theorem**

Now we are in the position to prove the turnpike property of singular arcs in case of the original optimal control problem with dynamics (3) and cost (2).

Theorem 5.2 *There exists a positive constant ϵ such that, if $z(\cdot)$ is singular and satisfies* (25) *on $[t_1, t_2] \subset [0, T]$, $\bar{z} = (\bar{z}_r, \bar{r})$ is the static point, solution of* (8)*, and if*

$$\|z(t_1) - \bar{z}\| + \|z(t_2) - \bar{z}\| \leq \epsilon \tag{29}$$

then there exists $C > 0$ such that for any $t \in [t_1, t_2]$ there holds

$$\|z(t) - \bar{z}\| + |u_s(t) - \bar{u}| \leq C\left(e^{\mu(t_1 - t)} + e^{\mu(t - t_2)}\right) \tag{30}$$

where $\mu = \frac{\bar{p}\bar{r}}{K+\bar{p}}$.

Proof. By Theorem 5.1, the singular trajectories in the original problem (3)-(2) and the reduced problem (4)-(2) coincide. As a consequence on Theorem 4.2, condition (29) implies: $|p_s(t) - \bar{p}| + |x_s(t) - \bar{x}| + |r_s(t) - \bar{r}| \leq C\left(e^{\mu(t_1-t)} + e^{\mu(t-t_2)}\right)$. Next, we are left to notice that the adjoint state λ is a rational function of (p, x, r) near the stationary point $(\bar{p}, \bar{x}, \bar{r})$ and the singular control u_s is a continuous function of (z, λ). This implies (30) up to a new constant C and ends the proof. □

In the case of optimal control problem (3)-(2), simulations show the predominance of the singular arcs and as a consequence, we observe the *turnpike* of the full solution as can be seem in Fig. 5 where the results are shown for increasing sequence of final times. As in the case of the reduced problem, we formulate a conjecture on the turnpike property the whole optimal solutions of (3)-(2).

Conjecture 5.1 Fix (p_0, x_0, r_0) in $(0, +\infty) \times (0, +\infty) \times [0, 1]$. There exists a constant $T_0 > 0$ such that for any $T > T_0$ and any optimal extremal $t \mapsto (z(t), \lambda(t))$ for problem (3)-(5) with initial condition (p_0, x_0, r_0), and with associated control $t \mapsto u(t)$, the following upper-bound holds for any t in $[0, T]$:

$$\|z(t) - \bar{z}\| + |u(t) - \bar{u}| \leq C\left(e^{-\mu t} + e^{\mu(t-T)}\right).$$

6 Suboptimal control strategies

6.1 Stability properties

In this section we show stability properties of the dynamical system obtained by taking the static value $\bar{r}$ in the reduced case and $\bar{u}$ in the complete case as a constant control. This control choice is particularly interesting because it permits to approximate the singular control as it is shown further in this section. The approximation of the singular control is further used in the design of numerical methods for both reduced and full problems. The stability properties justify the use of the constant control, that will allow reaching the turnpike exponentially fast, while it would absolutely not be the case without stability. Notice that in our case the singular control is given by a complicated rational function and the possibility to approximate this function by a simple constant control without a significant loss in the cost is especially valuable for application.

6.1.1 ***Reduced case***

We start the analysis of the stability properties by considering the case of the reduced problem (4), (2).

Theorem 6.1 *Assume $K = K_1$. Let $(\bar{p}, \bar{x}, \bar{r})$ be the solution of the static problem* (8) *and let (p, x) be the solution of* (4) *corresponding to $r \equiv \bar{r}$ and the initial data $(p(0), x(0)) = (p_0, x_0)$. Then there exist constants $\beta = \beta(p_0) > 0$ and $C = C(p_0, x_0) > 0$ such that the following inequality holds for any $t > 0$*

$$|p(t) - \bar{p}| + |x(t) - \bar{x}| \leq C\, e^{-\beta t}. \tag{31}$$

Proof. First let us denote $\psi(p) = \frac{p}{p+K}$. This function is strictly increasing and positive for $p > 0$. Remind if $r(t) = \bar{r}$ for $t \in [0, T]$ then $(\bar{p}, \bar{x})$ is the equilibrium of (4). This permits to rewrite (4) in the following form

$$\begin{aligned} \dot{p} &= -\frac{1}{p+K}\left(\frac{K\left(k_1\left(1-\bar{r}\right) + \bar{r}\left(1+\bar{p}\right)\right)}{\bar{p}+K} + \bar{r}p\right)\left(p - \bar{p}\right), \\ \dot{x} &= -\bar{r}\psi(p)\left(x - \bar{x}\right), \end{aligned} \tag{32}$$

which can be written in a simpler form as

$$\begin{aligned} \dot{p} &= -d_1(p)\left(p - \bar{p}\right), \\ \dot{x} &= -d_2(p)\left(x - \bar{x}\right). \end{aligned}$$

Coefficients d_1, d_2 have the following properties. First, $d_1(p) > d_1(0)$ for any $p > 0$ and $d_1(0) > 0$. Second, $d_2(p(t))$ is such that $d_2(p(t)) > d_2(p_0)$ if $p_0 < \bar{p}$ and $d_2(p(t)) > d_2(\bar{p})$ if $p_0 > \bar{p}$. Let us denote $V_p = |p(t) - \bar{p}|$, $V_x = |x(t) - \bar{x}|$. Outside $p = \bar{p}$ and $x = \bar{x}$, we have, $\dot{V}_p \leq -d_1 V_p$, and $\dot{V}_x \leq -d_2 V_x$, with $d_1 = d_1(0)$ and $d_2 = \min\{d_2(p_0), d_2(\bar{p})\}$. This is enough to deduce (31). □

In general there are no relations between K, K_1, so let us consider the case when $K = K_1$ is not necessarily satisfied. Without any assumption on parameters, the following Lemma holds.

Lemma 6.1 *Point $(\bar{p}, \bar{x})$ is the unique stable equilibrium of* (4) *with $r \equiv \bar{r}$ in Ω.*

Proof. The uniqueness is a consequence of the uniqueness of the equilibrium $(\bar{p}, \bar{r}, \bar{x})$ of (1). The linearized matrix of (4) is of the following form

$$\begin{pmatrix} -(\bar{p}+1)\mu_2'(\bar{p},\bar{r}) - \mu_2(\bar{p},\bar{r}) - \mu_1'(\bar{p},\bar{r}) & 0 \\ * & -\mu_1(\bar{p},\bar{r}) \end{pmatrix},$$

with $\mu_1 = \frac{k_1 p(1-r)}{K_1+p}$ and $\mu_2 = \frac{pr}{K+p}$. As $\mu_1(\bar{p},\bar{r}), \mu_2(\bar{p},\bar{r}), \mu_1'(\bar{p},\bar{r}), \mu_2'(\bar{p},\bar{r})$ are positive, both eigenvalues of the matrix above are negative. Therefore, $(\bar{p}, \bar{x})$ is a stable equilibrium. □

Let us denote by $(p_{\bar{r}}, x_{\bar{r}})$ the solution of (4) with constant control $r = \bar{r}$ defined on some time interval $[0, \widetilde{T}]$.

Lemma 6.2 *There exist $\delta,\ \overline{\mu},\ \overline{C} > 0$ such that if, $|p_{\bar{r}}(0) - \bar{p}| + |x_{\bar{r}}(0) - \bar{x}| \leq \delta$, then,*

$$|p_{\bar{r}}(t) - \bar{p}| + |x_{\bar{r}}(t) - \bar{x}| \leq \overline{C}\, e^{-\overline{\mu} t}, \quad \textit{for } t \in [0, \widetilde{T}].$$

Corollary 6.2. *There exist positive constants ϵ, T_0 such that, if $t_2 - t_1 > T_0$ and,*

$$|p_s(t_1) - \bar{p}| + |x_s(t_1) - \bar{x}| + |p_s(t_2) - \bar{p}| + |x_s(t_2) - \bar{x}| \leq \epsilon,$$

then there exists $C, C_J > 0$ such that for any $t \in [0, \widetilde{T}]$ there holds,

$$|p_s(t) - p_{\bar{r}}(t)| + |x_s(t) - x_{\bar{r}}(t)| + \leq C\left(e^{-\nu t} + e^{-\nu(\widetilde{T}-t)}\right),$$

and, $|J(r_s) - J(\bar{r})| \leq C_J\left(1 - e^{-\nu\widetilde{T}}\right)$.

6.1.2 ***Complete case (full model)***

Similar properties hold for the initial OCP (3), (2).

Lemma 6.3 *Point $(\bar{p}, \bar{r}, \bar{x})$ is the unique stable equilibrium of* (3) *with $u \equiv \bar{u}$ in Ω.*

Just as before, we denote by $(p_{\bar{u}}, r_{\bar{u}}, x_{\bar{u}})$ the solution of (4) with constant control $u \equiv \bar{u}$ defined on some time interval $[0, \widetilde{T}]$.

Lemma 6.4 *There exist $\delta,\ \overline{\mu}_*,\ \overline{C} > 0$ s.t if, $|p_{\bar{u}}(0) - \bar{p}| + |r_{\bar{u}}(0) - \bar{r}| + |x_{\bar{u}}(0) - \bar{x}| \leq \delta$, then, $|p_{\bar{u}}(t) - \bar{p}| + |r_{\bar{u}}(0) - \bar{r}| + |x_{\bar{u}}(t) - \bar{x}| \leq \overline{C}\, e^{-\overline{\mu}_* t},$ for $t \in [0, \widetilde{T}]$.*

Corollary 6.3. *There exist positive constants ϵ, T_0 such that, if $t_2 - t_1 > T_0$ and,*

$$|p_s(t_1) - \bar{p}| + |r_s(t_1) - \bar{r}| + |x_s(t_1) - \bar{x}| + |p_s(t_2) - \bar{p}| + |r_s(t_2) - \bar{r}| + |x_s(t_2) - \bar{x}| \leq \epsilon,$$

then there exists $C, C_J > 0$ such that for any $t \in [0, \widetilde{T}]$ there holds,

$$|p_s(t) - p_{\bar{u}}(t)| + |r_s(t) - r_{\bar{u}}(t)| + |x_s(t) - x_{\bar{u}}(t)| + \leq C\left(e^{-\nu t} + e^{-\nu(\widetilde{T}-t)}\right),$$

and, $|J(u_s) - J(\bar{u})| \leq C_J\left(1 - e^{-\nu\widetilde{T}}\right)$.

6.2 **Numerical algorithm for the reduced problem.**

Numerical solutions of the reduced problem obtained using direct method implemented in `Bocop` software show that, for different parameters K, K_1, k, E_M, different initial data (p_0, x_0) and different final times T, the obtained solutions are always with at most 3 arcs, see Section 3.1 for an example in case $E_M = k_1 = K_1 = K = 1$. Moreover, the solutions with exactly 3 arcs are the most frequent solutions and occur when final time is large. In case of 3-arcs solution, the observed structure is Bang-Singular-Bang (B-S-B). We will take advantage of this observation and assume in following that solutions of the reduced problem have at most 3 arcs and the sequence of the arcs is a sub-sequence of B-S-B. With this assumption, we will construct a new algorithm useful for applications, in which we will approximate the singular arc by a trajectory with the constant control $r = \bar{r}$, from the solution of the static problem (8).

Let us define a new optimisation problem associated with the reduced problem (5). We will use the notation $z^r = (p, x)$ and $\dot{z}^r = f_r(z^r, r)$ for the dynamics (4). We choose a control r in (4) in such a way that the dynamics takes the following form,

$$\begin{cases} \dot{z}^r = f_r(z^r, r_1), & t \in [0, T_1), \\ \dot{z}^r = f_r(z^r, \bar{r}), & t \in [T_1, T_2), \\ \dot{z}^r = f_r(z^r, r_2), & t \in [T_2, T], \end{cases} \tag{33}$$

where $\bar{r}$ is the solution of the *static*–OCP (8), r_1, r_2, T_1, T_2 are parameters satisfying $0 \leq r_1, r_2 \leq 1$ and $0 \leq T_1 \leq T_2 \leq T$. A reasonable next step is to find r_1, r_2, T_1, T_2 which maximize the cost (2) subject to (33). For this, we notice first that from the preliminary analysis in Section 4.1 it follows that the optimal control of the reduced OCP is zero during the final bang arc, meaning that $r \equiv 0$ on some time interval $[\tilde{t}, T]$. Therefore, we will set $r_2 = 0$, this will reduce the dimension of the optimisation problem. Finally, the new optimisation problem writes,

$$\max \int_0^T \frac{k_1}{x(t)} \frac{p(t)(1 - r(t))}{K_1 + p(t)} \mathrm{d}t \qquad \begin{cases} (p, x, r) \text{ satisfy (33)}, \\ 0 \leq r_1 \leq 1, \ r_2 = 0, \\ 0 \leq T_1 \leq T_2 \leq T. \end{cases} \tag{34}$$

Proposition 6.1 *The optimisation problem* (34) *admits a solution.*

Proof. Notice first that (34) is an optimisation problem where we maximize the cost with respect to 3 parameters r_1, T_1, T_2. This becomes apparent when we write (34) equivalently as follows,

$$\max_{\substack{0 \leq r_1 \leq 1 \\ 0 \leq T_1 \leq T_2 \leq T}} \int_0^{T_1} \frac{k_1}{x_{r_1}(t)} \frac{p_{r_1}(t)(1 - r_1)}{K_1 + p_{r_1}(t)} \mathrm{d}t + \int_{T_1}^{T_2} \frac{k_1}{x_{\bar{r}}(t)} \frac{p_{\bar{r}}(t)(1 - \bar{r})}{K_1 + p_{\bar{r}}(t)} \mathrm{d}t + \int_{T_2}^{T} \frac{k_1}{x_0(t)} \frac{p_0(t)}{K_1 + p_0(t)} \mathrm{d}t, \tag{35}$$

with the notation $(p_{r_*}(\cdot), x_{r_*}(\cdot))$ for the flow of (4) with control r set to be $r(\cdot) \equiv r_*$. Notice that the flow $(p_{r_*}(\cdot), x_{r_*}(\cdot))$ is a continuous function of r_*, therefore, the cost is a continuous function of r_1. Moreover, as T_1, T_2 only appear in the cost as the integral limits, the cost depends continuously on T_1, T_2. As a result, we maximize a continuous function on a compact set $\{(r_1, T_1, T_2) \ : \ 0 \leq r_1 \leq 1, \ 0 \leq T_1 \leq T_2 \leq T\}$. Such a maximization problem admits a solution. □

If we assume that the solutions of the reduced problem (4), (2) are of B - S - B structure, with the third arc corresponding to control $r(\cdot) \equiv 0$, then (34) approximates the solutions by replacing the middle arc by a constant value $r(\cdot) \equiv \bar{r}$. The idea of replacing a complicated singular control by a simple constant control is important for applications. By solving (34), we choose moreover the best control values and switching times for such a control structure. By Lemma 6.2 and Corollary 6.2, the behaviour of solutions of (4) with $r(\cdot) \equiv 0$ is very similar to the turnpike behaviour of the singular arc (approaches the static point exponentially fast), moreover, the error committed by setting the control $r(\cdot) \equiv \bar{r}$ in place of $r(\cdot) = r_s(\cdot)$ is bounded. The numerical simulations show even a better result when compared to the solutions obtained using the standard direct optimization method, see Section 7 for the comparison of the two methods. As shown in Sect. 7, the relative error is small, and for large T the 3-arc algorithm described above provide even better result.

For the numerical solution of (34) we use `Bocop` software with the option of maximization with respect to parameters and not the control function as it is done to solve standard DOCPs. In practice, this problem can be solved by any nonlinear programming solver. The discretization of the dynamical part of the constraint in (35) can be done in various ways just as in case of the direct methods for DOCPs (see [2] for direct methods in optimal control). We choose the approach of complete state discretization implemented in `Bocop`. In this case the differential equation becomes just a finite number of constraints in our nonlinear program. In the following numerical results we compare solutions of the reduced DOCP (5) obtained using direct method and the corresponding solutions of (34), to obtain both solutions we use `Bocop` software and the same discretization method. The comparison is done for the same parameters K, K_1, k, E_M, initial data (p_0, x_0) and final times T.

6.3 **Numerical algorithm for the original problem.**

The idea of approximating solutions with a simple piecewise constant control strategy which was described in case of the reduced problem applies in case of the original problem (3), (2) with small modifications. From PMP it follows that $H_1(T) = 0$, so we can not conclude on the exact value of the control during the final arc as it was done in the reduced case. Therefore, if we approximate a solution with 3 consecutive constant controls, the value of the last control remains an optimisation parameter. We use the notation $z = (p, r, x)$ and $\dot{z} = f(z, u)$ for the dynamics (3). The 3-arcs strategy leads to the following dynamics with $\bar{u}$ the corresponding value from the solution of the static problem.

$$\begin{cases} \dot{z} = f(z, u_1), & t \in [0, T_1) \\ \dot{z} = f(z, \bar{u}), & t \in [T_1, T_2) \\ \dot{z} = f(z, u_2), & t \in [T_2, T]. \end{cases} \tag{36}$$

The resulting optimization problem has the following form.

$$\max \int_0^T \frac{k_1}{x(t)} \frac{p(t)(1 - r(t))}{K_1 + p(t)} \mathrm{d}t, \quad s.t., \quad \begin{cases} (p, x, r) \text{ satisfy (36)}, \\ 0 \leq u_1, u_2 \leq 1, \\ 0 \leq T_1 \leq T_2 \leq T \end{cases} \tag{37}$$

Using the same arguments as in the proof of Proposition 6.1, we get the existence of a solution of (37).

Proposition 6.2 *The optimisation problem* (37) *admits a solution.*

Solution's structure of the complete optimal control problem (3), (2) is more complicated than in the reduced case as the connection between bang arcs and singular arcs is achieved by chattering. It is standard to approximate chattering by finite number of bang arcs in numerical methods, see [25], but there is no general theory on such an approach, the method should be adapted to the concrete problem under consideration. Assume that all optimal solutions of problem (3), (2) have only one singular arc. In this case, the 3-arcs solution represents an approximation where all the bang-arcs, including chattering, before and after the singular arc are replaced by a single arc corresponding to a constant control, and the singular arc is approximated by an arc corresponding to the control $u = \bar{u}$. Notice that solution of (3) with $u = \bar{u}$ converges exponentially to $\bar{z}$, and thus, is exponentially close to the singular arc, just as in the reduced case as shown in Corollary 6.3. In the following numerical results we confirm that the numerical solution of (37) approximate well the numerical solution of the complete optimal control problem (3), (2) in both cases solutions are compared to the results of the direct method and are obtained using `Bocop` .

7 Numerical results

In this section, we provide various implementation results and numerical examples exploiting the generic algorithms established in Sections 6.2, 6.3. For that, we use the open source optimal control toolbox `Bocop`. The results obtained using 3-arc algorithms are compared to the standard direct optimization approach implemented also in `Bocop`. Note that the introductory examples developed in Section 3 rely upon the direct optimization method as well and are realized using `Bocop`.

E_M	k_1	K_1	K
2.5	1.2	1.4	1.6

Table 2: Numerical values of the parameters of the model (4), used in the illustrations in *Examples 1-2* in Sect. 7, for the reduced problem. In this case, we note that $\overline{u} = \overline{r}$, the *static* solution of the *static*-OCP (9), is given by $\overline{u} = \overline{r} = 0.6$.

Example 7.1 **[Reduced self-replicator model]**
In the first numerical example, we illustrate the model behavior (using the parameters in Tab. 2 along with the

Bocop settings[3] and we provide the optimal state and co-state trajectories, along with the optimal control $r(t)$, using a direct optimization method applied to the reduced DOCP. These solutions clearly exhibit a *turnpike* behavior, associated with the singular arc regime, as illustrated in Fig. 6-7.

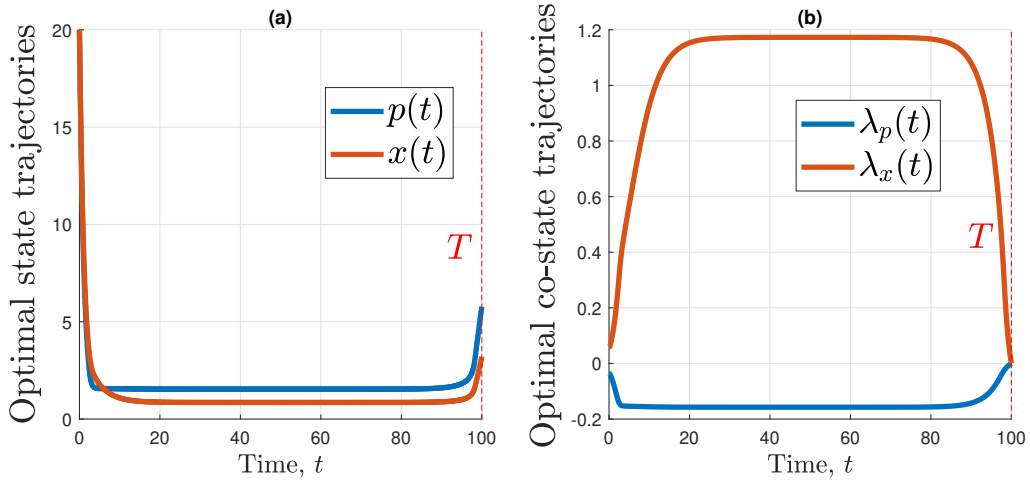

Fig. 6: **(a)** The optimal $p(t)$ and $r(t)$ over $[0, 100]$, associated with the control given in Fig. 7. The control is provided by Bocop, numerically using a direct method solving the reduced DOCP. The initial states are given by $p(0) = x(0) = 20$. **(b)** The optimal co-state trajectories $\lambda_p(t)$ and $\lambda r(t)$ over $[0, 100]$, associated with the control given in Fig. 7. We note that the transversality conditions (from the PMP) are satisfied.

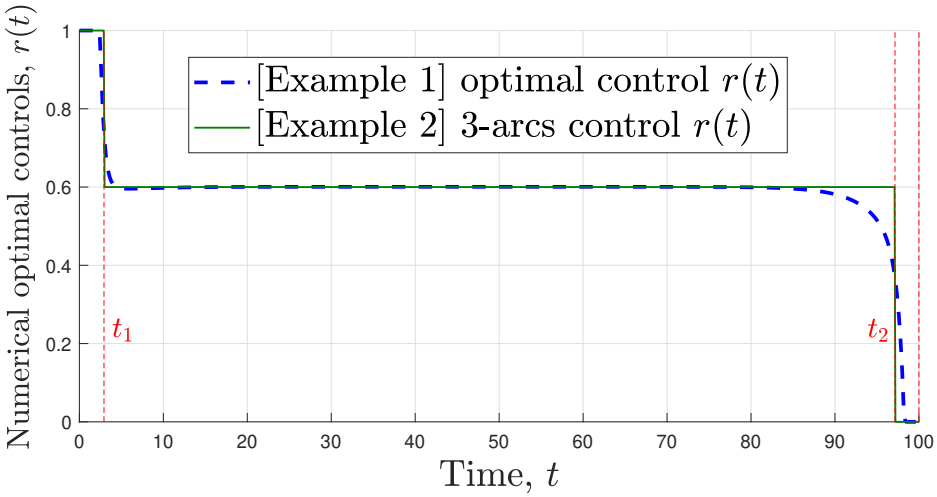

Fig. 7: The numerical optimal control $r(t)$, over $[0, 100]$, derived from the reduced DOCP (Example 1), compared to the 3–arcs approximation (Example 2). The 3–arcs sub-optimal control consists of three pieces: r_1 (active over $[0, t_1]$, with $t_1 = 2.9288$) which is set to be free in the optimization algorithm, *i.e.* r_1 as t_1 and t_2 are the optimization variables. Then, the phase of the control over $[t_1, t_2]$, where the optimized t_2 is given by $t_2 = 97.1477$, which is the *static* point $r_2 = \bar{r} = 0.6$. Finally, the control r_3 is set to zero in this problem (from the PMP necessary conditions).

[3] Numerical experiments were run on bocop when T ranges from 20 to 280 (see Tab. 3), with the following settings. Discretization: Euler (implicit, 1-stage, order 1), time steps: 500, Maximum number of iterations: 2000, NLP solver tolerance: 10^{-18}.

Example 7.2 **[Reduced self-replicator model – 3-arcs]**
Now, we consider the numerical method based on the 3 arcs approximation, considering the reduced problem, using the `Bocop` settings[4]. Indeed, the results provided in Example 1 clearly show the relevance of the use of constant control $\overline{r}$ during the singular regime. First, let us show for $T = 100$ the sub-optimal control and the sub-optimal trajectories illustrated, respectively, in Fig. 7 and 8, obtained using the model parameters in Tab. 2. Next, we obtained several numerical results for different final-times T, in order to compare the standard direct numerical approach and the approach by the 3-arcs algorithm. The results are given in Tab. 3. The comparison is done by considering the relative error of the numerically obtained value functions of the two algorithms, that is the maximal cost value, for different final times, $\epsilon(T) = \frac{C_{3-arcs}(T)-C_{DOCP}(T)}{C_{DOCP}(T)}$, where $C_{DOCP}(T)$ is the maximal value of the cost obtained using standard direct approach and $C_{3-arcs}(T)$ is the value obtained by the 3-arc algorithm, the both values are considered as functions of the final time T. Notice that we do not take the absolute value of difference, $C_{3-arcs}(T) - C_{DOCP}(T)$. This is done in order to capture which cost provides the better result at each time T. Notice that the considered OCPs are formulated as a maximization problems. Thus, if the values of $\epsilon(T)$ is positive then the maximal cost value obtained by the 3-arc algorithm is larger than the value obtained by the direct method. This indicates the better performance of the control strategy obtained by the 3-arc algorithm for this concrete time choice T. In the same way, the negative values of $\epsilon(T)$ imply the better performance of the direct method for the corresponding values T. As we showed further both for the reduced and the complete models, the 3–arc algorithms show the better performance when T grows.

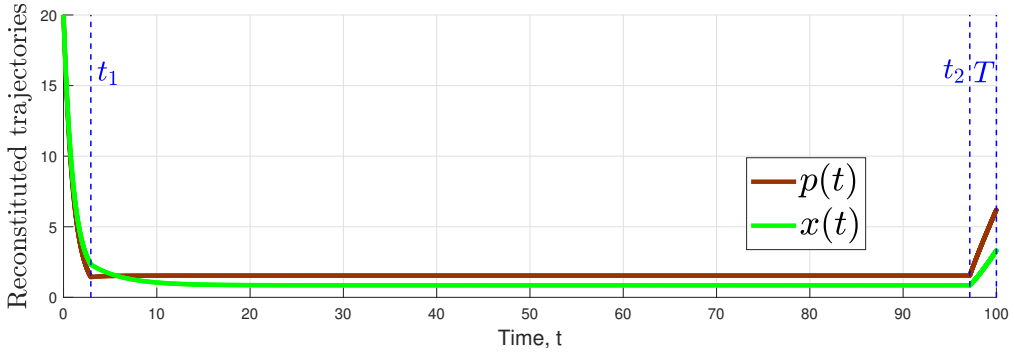

Fig. 8: These are the reconstituted sub-optimal trajectories $p(t)$ and $x(t)$ in the 3–arcs method, steered over $[0, 100]$ by the sub-optimal control $r(t)$ given in Fig. 7. We recall that the optimized time-switching instants are given by $t_1 = 2.9288$ and $t_2 = 97.1477$. The initial conditions in this case are given by, $p(0) = x(0) = 20$.

T	20	40	60	80	100	120	140
Reduced DOCP cost	10.3791	16.2434	22.1082	27.9735	33.8393	39.7055	45.5721
Reduced $\text{Cost}_{3-\text{arcs}}$	10.4107	16.2974	22.1841	28.0709	33.9578	39.8447	45.7317
T	160	180	200	220	240	260	280
Reduced DOCP cost	4.52314	51.439	57.3062	63.174	69.0418	74.91	80.7786
Reduced $\text{Cost}_{3-\text{arcs}}$	4.53117	51.6188	57.5058	63.3929	69.2801	75.1673	81.0545

Table 3: The cost associated to the numerical methods: DOCP cost stands for the direct optimization solving the initial DOCP, and Cost_{3-arcs} gives the cost of the numerical method fixing the singular regime to $\overline{r}$.

Clearly, as illustrated in Tab. 3 and Fig. 9, the costs of the numerical direct method solving the reduced original DOCP and the numerical algorithm based on the 3-arcs approach, are substantially similar. We even note in this case that the maximization achieved by the 3-arcs algorithm is slightly better than the free `Bocop` case when the final-time increases. These comparative results were obtained for equivalent numerical discretization methods and may slightly vary according to the selected ODE-discretization schemes.

[4] Numerical experiments were run on `bocop` for $T = 70$ (time unit), with the following settings. Discretization:`Lobatto IIIC (implicit, 4-stage, order 6)`, time steps: 500, Maximum number of iterations: 2000, NLP solver tolerance: 10^{-18}.

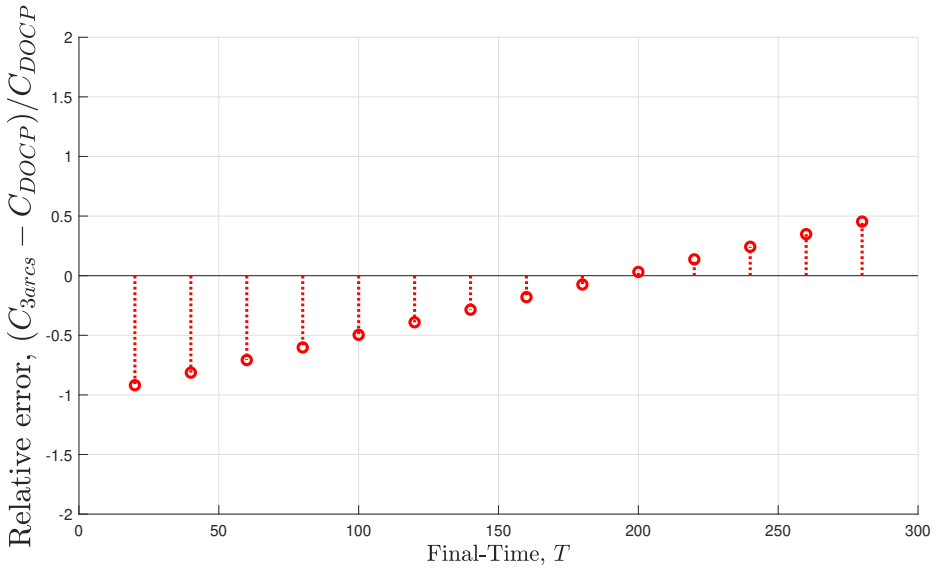

Fig. 9: Using the data in Tab. 3, the relative error characterizing the use of the two numerical method is represented for T, the final-time, varying between 20 and 280. The cost C_{DOCP} stands for the direct optimization in `Bocop`, while C_{3-arcs} stands for the cost using the 3 arcs approach. The second method is clearly more efficient when T becomes large. The comparison is made on the basis of equivalent *Bocop* settings.

Let us now perform similar numerical examples based on the dynamics of the full model (3). The biological parameters in this case are given in Tab. 4. The results obtained in Examples 7.3-7.4 using appropriate `Bocop` settings are summarized in Tab. 6 in Appendix B.

E_M	k_1	K_1	K
2	1.2	1.4	1.6

Table 4: Numerical values of the biological parameters of the models (3)-(4) used in the numerical illustrations in Section 7 in *Examples 3-4* for the full problem. In this case, we note that $\overline{u}$, the *static* solution of the *static*-OCP, is given by $\overline{u} = 0.58$.

Example 7.3 **[Full self-replicator model]**
Firstly, we illustrate for a fixed final-time $T = 70$ the model behavior and provide the optimal state trajectories, co-state trajectories and the associated optimal control $u(t)$, using a direct optimization method applied to the complete DOCP. A chattering phenomenon appears in the optimal control in Fig. 10. As in the reduced problem, these solutions clearly exhibit the *turnpike*-type behavior, associated with the singular arc regime, as illustrated in Fig. 10-11.

In the last numerical example, we apply the 3-arcs based algorithm to the full problem. For that we perform several numerical simulations for different final-times T, given in Tab. 4.

Example 7.4 **[Full self-replicator model — Solution with the 3-arcs algorithm]**
Now, we consider the full model (3), associated with the 3-arcs optimization problem (37). The biological parameters are given in Tab. 4, implemented in `Bocop` along with the `Bocop` settings[5]. The results when T varies from 70 to 470 are listed in Tab. 6.

❒ **Results for** $T = 70$**:**

[5] Numerical experiments were run on `bocop`, when T ranges from 70 to 470 (see Tab. 6), with the following settings. Discretization: Euler (implicit, 1-stage, order 1), time steps: 500, Maximum number of iterations: 2000, NLP solver tolerance: 10^{-20}.

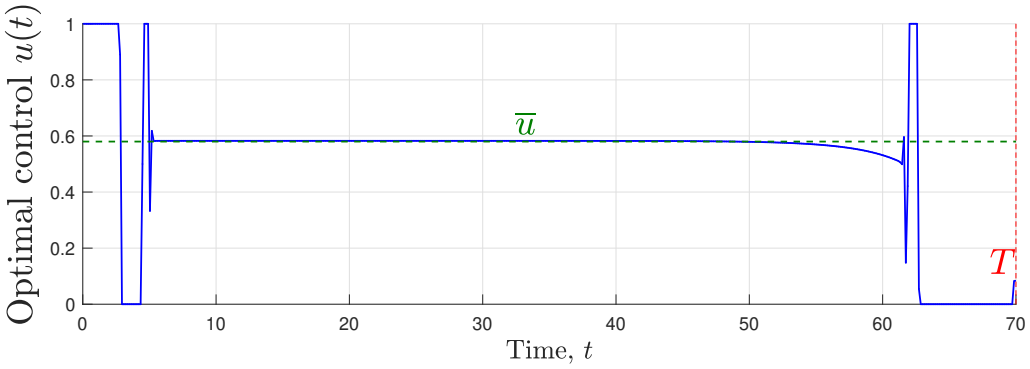

Fig. 10: The optimal control $u(t)$ over $[0, 70]$ in Example 3.

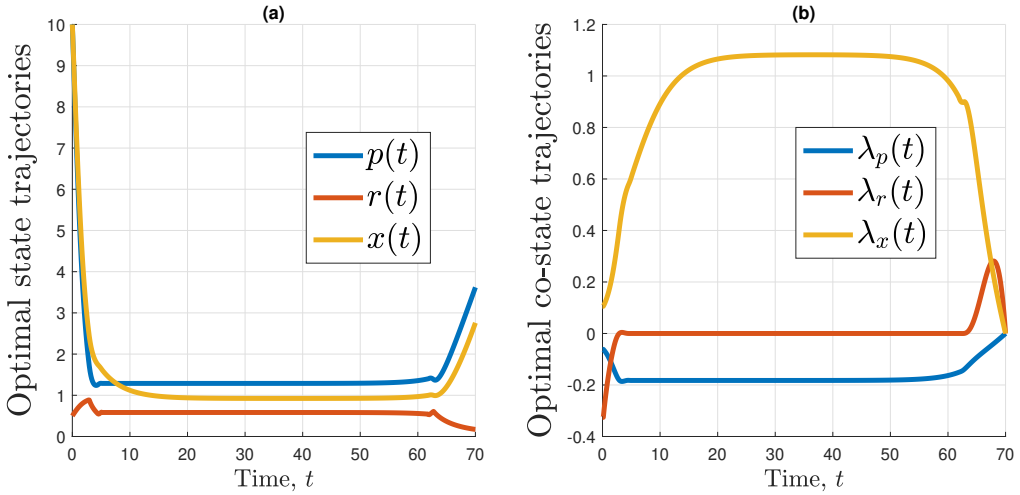

Fig. 11: The optimal state trajectories (a) and co-state trajectories (b) corresponding to the optimal control given in Fig. 10. The trajectories in (a)-(b) exhibit as expected the turnpike-type behavior. Notice also that the transversality conditions (*i.e.,* $\lambda(T) = 0$ from the PMP) are satisfied in (b).

The (sub)optimal control using the 3-arcs is given in Fig. 12. The corresponding reconstituted model trajectories are given in Fig. 13.

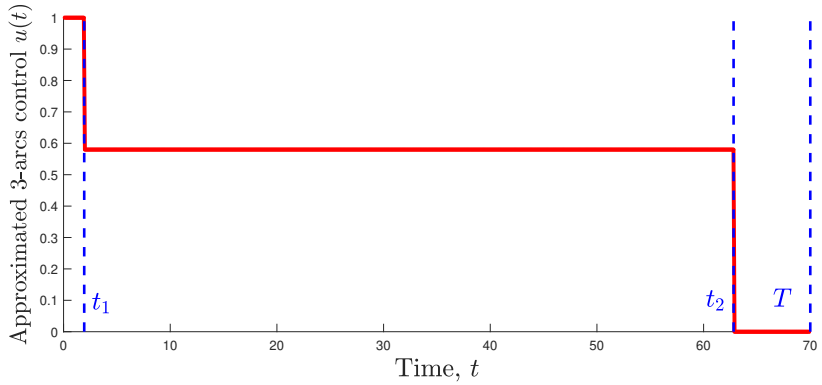

Fig. 12: The reconstituted optimal 3-arcs (sub)optimal control $u(t)$ for $t \in [0, 70]$. In this case $u_2 = \overline{u} = 0.58$. See Tab. 6 for values of t_1, t_2 and the corresponding cost.

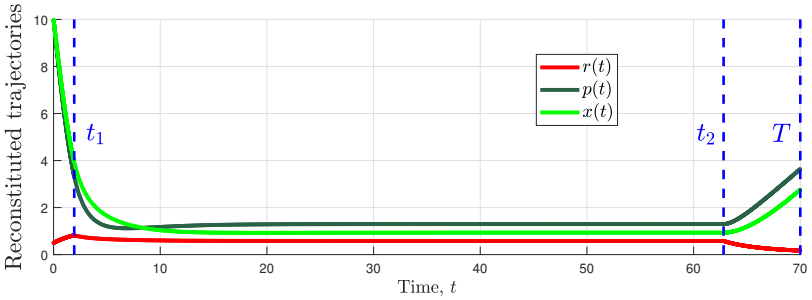

Fig. 13: The reconstituted (sub)optimal trajectories resulting from the 3-arcs approach, derived from the (sub)optimal control $u(t)$ given in Fig. 12 for $t \in [0, 70]$.

❒ **Results for** $T = 470$**:**

The control obtained using the 3-arcs algorithm is given in Fig. 14. The corresponding reconstituted model trajectories are given in Fig. 15.

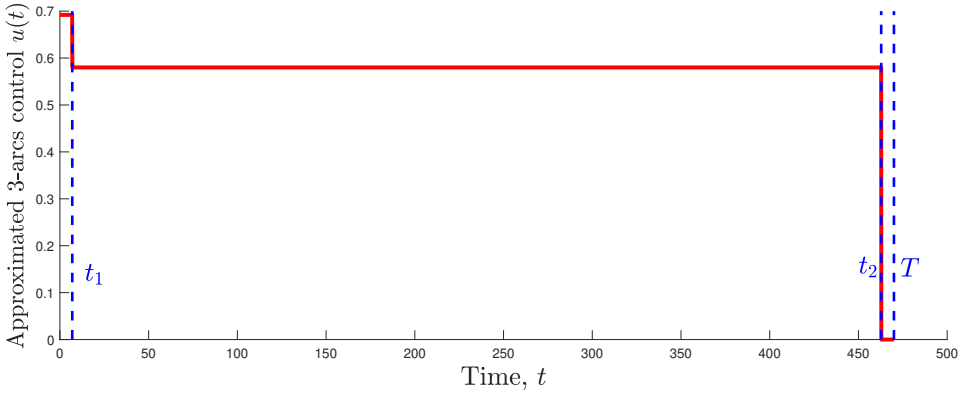

Fig. 14: The reconstituted optimal 3-arcs control $u(t)$ for $t \in [0, 470]$. In this case $u_2 = \overline{u} = 0.58$. See Tab. 6 for the values of t_1, t_2 and the corresponding cost.

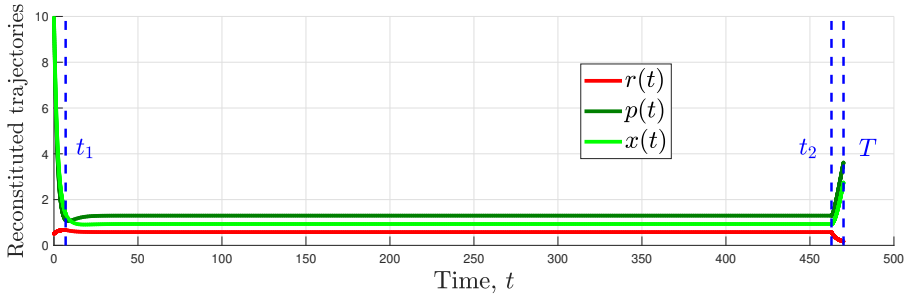

Fig. 15: The reconstituted (sub)optimal trajectories resulting from the 3-arcs approach, derived from the (sub)optimal control $u(t)$ given in Fig. 14 for $t \in [0, 470]$.

Using the data given in Tab. 6, we deduce the relative error committed between the two numerical methods is substantially minor. The difference increases slowly when T is very large to the favor of the effective three arcs approximation. Indeed, we note that when T increases, the approximated 3-arcs algorithm has better yields

than the original DOCP (for equivalent discretization method and same time-steps in Bocop). However, overall, the results of both numerical methods are substantially similar, which comforts strongly the use of the simplest sub-optimal control as an alternative effective control strategy.

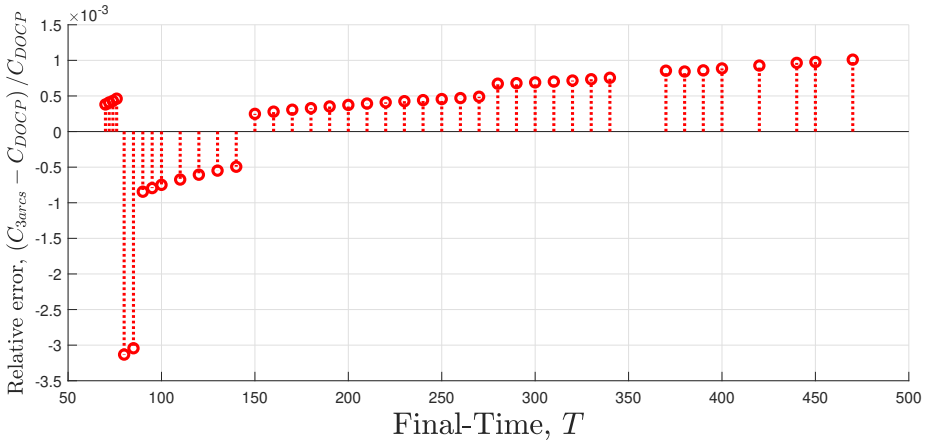

Fig. 16: The relative error in the costs committed when T varies from 70 to 470. The comparison is made on the basis of the *Bocop* settings given in Appendix B.

8 Conclusion

We made the first steps in showing the *turnpike* property of the optimal solutions. We extended the existing theoretical approach from [18] on the local exponential *turnpike* property to our case with the singular arcs. The Pontryagin maximum principle together with numerical methods permitted us to deduce the possible structure of the solutions with predominance of the singular arc. In addition, we introduced the reduced model which permits to avoid the chattering phenomenon. Finally, we designed simple sub-optimal open loop strategies for both reduced and complete models. These strategies are easier to implement from a biological and experimental point of view. The efficiency of the method was shown on numerical examples. For future work, we will further use the solution of the reduced OCP for construction of the control strategies for the original OCP. The other direction on which we will focus is the establishment of global *turnpike* behavior in the studied class of OCPs dedicated to bacterial growth, in particular using dissipativity features [10, 14].

Acknowledgements. This research work has received most support from the ANR Project Maximic (**ANR-17-CE40-0024**), and also benefited from the support of the ANR PhotoBiofilm Explorer (**ANR-20-CE43-0008**). The authors are grateful to Laetitia Giraldi and Agustin Yabo from Inria, and also Térence Bayen from Avignon University for fruitful exchanges about singular arcs and *turnpike* phenomena.

References

1. A. Agrachev., & Y. Sachkov. *Control Theory from the Geometric Viewpoint.* Encyclopaedia of Mathematical Sciences, Springer- Verlag (87), 2004.
2. J.T. Betts, *Practical methods for optimal control and estimation using nonlinear programming*. Siam, Advances in Design & Control, 2nd Edition, Vol. 19, 2010.
3. L.T. Biegler, *Nonlinear Programming: Concepts, Algorithms, and Applications to Chemical Processes*. MPS-SIAM Series on Optimization (Book 10), SIAM, 2010.
4. B. Bonnard., & M. Chyba. *Singular trajectories and their role in control theory*. Springer Science & Business Media (40), 2003.
5. J.-B. Caillau, W. Djema, L. Giraldi, J.-L. Gouzé, S. Maslovskaya, J.-B. Pomet. *The turnpike property in maximization of microbial metabolite production*. IFAC World Congress, 2020.
6. M. Caponigro, R. Ghezzi, B. Piccoli., E. Trélat. *Regularization of Chattering Phenomena via Bounded Variation Controls* IEEE Transactions on Automatic Control, vol. 63, no. 7, 2046-2060, 2018.
7. W. Djema, L. Giraldi, S. Maslovskaya, O. Bernard., *Turnpike features in optimal selection of species represented by quota models* Automatica, 2021.

8. K. Ezal, Z. Pan, P.V. Kokotovic, *Locally optimal and robust backstepping design*. IEEE transactions on automatic control, 45(2), 260–271, 2000.
9. T. Faulwasser, & L. Grüne., *Turnpike properties in optimal control: An overview of discrete-time and continuous-time results.*, arXiv preprint arXiv:2011.13670., 2020.
10. T. Faulwasser, M. Korda, C.N. Jones, D. Bonvin, *On turnpike and dissipativity properties of continuous-time optimal control problems*. Automatica, 81, 297–304, 2017.
11. N., Giordano., F. Mairet, J.-L. Gouzé, J. Geiselmann, and H. De Jong, *Dynamical allocation of cellular resources as an optimal control problem: novel insights into microbial growth strategies.*, PLoS computational biology, 12(3), e1004802, 2016.
12. P. Kokotović, H.K. Khalil, J. O'Reilly, *Singular perturbation methods in control*. SIAM, 1986.
13. D. Molenaar, D. van Berlo, D. de Ridder, B. Teusink, *Shifts in growth strategies reflect tradeoffs in cellular economics.*, Mol Syst Biol. 5:323, pmid:19888218, 2009.
14. M.A. Müller, L. Grüne, F. Allgöwer, *On the role of dissipativity in economic model predictive control.*, IFAC-PapersOnLine, 48(23), 110-116, 2015.
15. D. Pighin, & A. Porretta, *Long time behaviour of Optimal Control problems and the Turnpike Property*. Master's Thesis, Thesis Università Degli Studi di Roma Tor Vergata, 2016.
16. L.S. Pontryagin, V.G. Boltyansky, R.V. Gamkrelidze, E.F. Mishchenko *The mathematical theory of optimal processes*. Macmillan, New York, 1964.
17. Team Commands, Inria Saclay, *BOCOP: an open source toolbox for optimal control*. `http://bocop.org`, 2019.
18. E. Trélat., & E. Zuazua., *The turnpike property in finite-dimensional nonlinear optimal control*. Journal of Differential Equations, 258(1), 81–114, 2015.
19. E. Trélat., & C. Zhang, *Integral and measure-turnpike properties for infinite-dimensional optimal control systems.* Mathematics of Control, Signals, and Systems, 30(1), 1–34, 2018.
20. S. Waldherr, D.A. Oyarzún, A. Bockmayr, *Dynamic optimization of metabolic networks coupled with gene expression.*, J Theor Biol. 365:469–85. pmid:25451533, 2015.
21. A. Yabo, J.-B. Caillau, J.-L. Gouzé *Singular regimes for the maximization of metabolite production*, 31–36 Proceedings of the 58th IEEE Conference on Decision and Control CDC, 2019.
22. A. Yabo, J.-B. Caillau, J.-L. Gouzé. *Optimal bacterial resource allocation: metabolite production in continuous bioreactors*. Mathematical Biosciences and Engineering, 17(6), 7074–7100, 2020.
23. I. Yegorov, F. Mairet, H. De Jong, J.-L. Gouzé. *Optimal control of bacterial growth for the maximization of metabolite production*. Journal of mathematical biology, 1–48, 2016.
24. M.T. Zelikin, & V.F. Borisov *Singular optimal regimes in problems of mathematical economics.* J Math Sci 130(1):4409–4570, 2005.
25. J. Zhu, E. Trélat, M. Cerf. *Planar tilting maneuver of a spacecraft: singular arcs in the minimum time problem and chattering*. Discrete & Continuous Dynamical Systems—B, 21–4, 1347–1388, 2016.

A Bocop settings and results used in Section 3.1

T	10	15	18	20	24	26	28	–
t_1	2.47	2.50	2.60	2.62	2.64	2.64	2.65	–
t_2	62.01	6.67	11.67	14.69	16.72	20.73	22.77	–
T	30	35	40	45	50	55	60	65
t_1	2.63	2.64	2.59	2.56	2.52	2.50	2.53	2.52
t_2	26.82	31.85	36.88	41.94	47.00	52.03	57.00	
T	70	80	90	100	120	125	135	150
t_1	2.52	2.40	2.34	2.40	2.40	2.25	2.16	2.10
t_2	67.06	77.12	87.12	97.20	117.36	122.25	132.30	147.60
T	200	230	250	280	300	310	320	–
t_1	2.00	1.84	2.00	1.68	1.80	1.86	1.90	–
t_2	197.60	227.70	248.00	277.76	298.20	308.14	318.08	–

Table 5: The values of the switching instants t_1 and t_2 for different time horizons $[0, T]$, where T ranges from 10 to 320.

B 3–arcs optimization results in the full-model

T	u_1	u_2	u_3	t_1	t_2	$\text{Cost}_{3-\text{arcs}}$	DOCP cost
70	1	0.58	0	1.9364	62.8107	17.0796	17.0731
72	1	0.58	0	1.9380	64.8107	17.5989	17.5917
74	1	0.58	0	1.9397	66.8108	18.1181	18.1103
76	1	0.58	0	1.9413	68.8108	18.6374	18.6288
80	1	0.58	0	2.1631	72.8469	19.6044	19.6660
85	1	0.58	0	2.1820	77.8477	20.8987	20.9625
90	1	0.58	0	2.0482	82.8231	22.2403	22.2591
95	1	0.58	0	2.0580	87.8234	23.5369	23.5556
100	1	0.58	0	2.0679	92.8237	24.8335	24.8521
110	1	0.58	0	2.0872	102.8242	27.4267	27.4452
120	1	0.58	0	2.1066	112.8246	30.0201	30.0383
130	1	0.58	0	2.1261	122.8251	32.6136	32.6315
140	1	0.58	0	2.1456	132.8256	35.2072	35.2246
150	1	0.58	0	2.0745	142.8175	37.8272	37.8178
160	1	0.58	0	2.0877	152.8177	40.4224	40.4111
170	1	0.58	0	2.1009	162.8179	43.0175	43.0043
180	1	0.58	0	2.1131	172.8181	45.6127	45.5977
190	1	0.58	0	2.1263	182.8183	48.2080	48.191
200	1	0.58	0	2.1395	192.8185	50.8033	50.7843
210	1	0.58	0	2.1517	202.8187	53.3987	53.3777
220	1	0.58	0	2.1649	212.8189	55.9941	55.9711
230	1	0.58	0	2.1771	222.8191	58.5896	58.5646
240	1	0.58	0	2.1903	232.8193	61.1850	61.158
250	1	0.58	0	2.2025	242.8195	63.7806	63.7515
260	0.9774	0.58	0	2.3202	252.8202	66.3762	66.345
270	0.9044	0.58	0	2.7646	262.8226	68.9722	68.9385
280	1	0.58	0	2.1922	272.8172	71.5802	71.5321
290	1	0.58	0	2.2034	282.8173	74.1762	74.1258
300	0.9867	0.58	0	2.2748	292.8178	76.7723	76.7193
310	0.9202	0.58	0	2.6536	302.8195	79.3686	79.3129
320	0.8648	0.58	0	3.0923	312.82137	81.9653	81.9066
330	0.8222	0.58	0	3.5538	322.8228	84.5624	84.5003
340	0.7917	0.58	0	3.9899	332.8239	87.1598	87.094
370	0.7856	0.58	0	4.0906	362.8226	94.9563	94.8752
380	0.7324	0.58	0	5.3045	372.8265	97.5512	97.469
390	0.7246	0.58	0	5.5538	382.8268	100.1490	100.063
400	0.7181	0.58	0	5.7811	392.8271	102.7480	102.657
420	0.7080	0.58	0	6.1835	412.8275	107.9440	107.844
440	0.7004	0.58	0	6.5278	432.8279	113.1410	113.032
450	0.6973	0.58	0	6.6830	442.8280	115.7390	115.626
470	0.6920	0.58	0	6.9632	462.8282	120.936	120.814

Table 6: Here we use the optimization method based on the 3–arcs, where u_2 is fixed to the *static* solution $u_2 = \overline{u}$ (where $\overline{u} = 0.58$ is the solution of the *static*-OCP in the full model, corresponding to the parameters in Tab. 4), while u_1 and u_3 are free. The optimal solution provided by `Bocop` reveals that u_3 is always zero. The last phase is characterized by $\beta = T_f - t_2$, on which $u_3 = 0$ is active, does not vary significantly when the final-time T ranges from 70 to 470. On the other hand, the singular phase over $\alpha = t_2 - t_1$, during which the control is exactly fixed to $\overline{u} = u_2 = 0.58$, increases significantly with respect to T. We also notice that the first phase covering $[0, t_1]$ has an optimal control $u_1 = 1$ from $T = 70$ to approximately 260, then the optimal u_1 is slowly decreasing while t_1 is slowly increasing w.r.t. T.